

DTIC FILE COPY

NASA CR-179582

AD-A183 088



National Aeronautics and
Space Administration

AVIATION FUEL PROPERTY EFFECTS ON ALTITUDE RELIGHT

Final Report

by

K.S. Venkataramani

GENERAL ELECTRIC COMPANY
Aircraft Engine Business Group
Cincinnati, Ohio 45215

Prepared for

National Aeronautics and Space Administration

Lewis Research Center
21000 Brookpark Road
Cleveland, Ohio 44135

This document has been approved
for public release and sale; its
distribution is unlimited.

NASA Lewis Research Center
Contract NAS3-24215

DTIC
ELECTE
JUL 27 1987
S D
E

1. Report No. CR-1/9582		2. Government Accession No. ADA183088		3. Recipient's Catalog No.	
4. Title and Subtitle Aviation Fuel Property Effects on Altitude Relight				5. Report Date May 1987	
				6. Performing Organization Code	
7. Author(s) K. Venkateramani				8. Performing Organization Report No. R87AEB111	
9. Performing Organization Name and Address GE Aircraft Engine Business Group Aircraft Engine Business Group Evendale, Ohio 45215				10. Work Unit No.	
				11. Contract or Grant No. NAS3-24215 5505-69-41	
12. Sponsoring Agency Name and Address NASA Lewis Research Center 21000 Brookpark Road Cleveland, Ohio 44135 (Joint program with Navy, Air Force, Army)				13. Type of Report and Period Covered Contractor Final Report January 84 - June 86	
				14. Sponsoring Agency Code	
15. Supplementary Notes Project Manager; J.A. Bieglow, NASA Lewis Research Center Unconventional Systems Branch 21000 Brookpark Road Cleveland, Ohio 44135					
16. Abstract <p>The major objective of this experimental program was to investigate the effects of fuel property variation on altitude relight characteristics.</p> <p>Four fuels with widely varying volatility properties (JP-4, Jet A and 2040 Solvent, and Diesel 2) were tested in a five-swirl-cup-sector combustor at inlet temperatures and flows representative of windmilling conditions of turbofan engines.</p> <p>The effects of fuel physical properties on atomization were eliminated by using four sets of pressure-atomizing nozzles designed to give the same spray Sauter mean diameter ($50 \pm 10 \mu\text{m}$) for each fuel at the same design fuel flow. A second series of tests was run with a set of air-blast nozzles.</p> <p>With comparable atomization levels, fuel volatility assumed only a secondary role for first-swirl-cup lightoff and complete blowout. Fuel propagation and first-cup blowout were independent of fuel volatility and depended only on the combustor operating conditions.</p> <p style="text-align: right;"><i>Keywords:</i></p>					
17. Key Words (Suggested by Author(s)) Gas Turbine Combustion , Altitude Relight , Ignition , Fuel Property Effects ←				18. Distribution Statement General Release	
19. Security Classif. (of this report) Unclassified		20. Security Classif. (of this page) Unclassified		21. No. of Pages 50	
22. Price					

FOREWORD

This final report documents the experimental program performed by the GE Aircraft Engine Business Group under NASA Contract NAS3-24215. The NASA Program Manager was Mr. James A. Biaglow. The GE Program Manager was Mr. Edward E. Ekstedt, and the principal investigator was Dr. K.S. Venkataramani.

Mr. Biaglow provided valuable guidance throughout the program. The efforts of Ms. Sara Murray, Messrs. Jerry Horton, Paul Ogden, James Poynter, Howard Gregory, Bill Keith, Mark Kelsey, Jerry Wheeler, Carl Woodruff, Mrs. Virginia Cecil, and Mrs. Laurie Hake are gratefully acknowledged.

Accession For	
NTIS GRA&I	<input checked="checked" type="checkbox"/>
DTIC TAB	<input type="checkbox"/>
Unannounced	<input type="checkbox"/>
Justification	
By	
Distribution/	
Availability Codes	
Dist	Avail and/or Special
A-1	

TABLE OF CONTENTS

<u>Section</u>		<u>Page</u>
1.0	SUMMARY	1
2.0	INTRODUCTION	2
3.0	TEST FUELS AND FUEL NOZZLES	7
3.1	Test Fuels	7
3.2	Fuel Nozzles	10
3.2.1	Pressure-Atomizing Nozzles	10
3.2.2	Prefilming Air-Blast Nozzles	10
4.0	TEST FACILITIES	14
4.1	Droplet-Measurement Facility	14
4.2	Test Combustor	14
4.3	Altitude-Relight Rig	16
4.3.1	Air-Cooling System	22
4.3.2	Fuel-Cooling System	22
5.0	TEST PROCEDURES	25
5.1	Droplet Measurement	25
5.2	Altitude Relight	26
6.0	TEST RESULTS	28
6.1	Droplet Measurement	28
6.2	Altitude-Relight and Lean-Blowout	29
6.2.1	Pressure-Atomizing Nozzle	29
6.2.1.1	Initial Lightoff	30
6.2.1.2	Full Propagation	30
6.2.1.3	First-Cup Blowout	41
6.2.1.4	Complete Blowout	41
6.2.2	Air-Blast Nozzle	41
7.0	CONCLUDING REMARKS	58
8.0	REFERENCES	59

LIST OF ILLUSTRATIONS

<u>Figure</u>		<u>Page</u>
1.	Reference Engine Altitude Relight Map; Combustor Airflows and Inlet Pressures Under Windmilling Conditions.	4
2.	Reference Engine Altitude Relight Map; Combustor Airflows and Inlet Temperatures Under Windmilling Conditions.	5
3.	Pressure-Atomizing Nozzle.	11
4.	Test Combustor Fuel Injector Schematic.	11
5.	Air-Blast Fuel Nozzle, Tip Details.	12
6.	Photographs of Air-Blast Fuel Nozzle.	13
7.	Spectron Droplet-Sizing Interferometer.	15
8.	Spectron Droplet-Sizing Interferometer Operating Principle.	15
9.	Schematic of the Combustor.	16
10.	Photo of Sector Combustor Looking Forward Into Dome.	17
11.	Sector Combustor Assembly.	18
12.	Front View of Dome.	19
13.	Altitude-Relight Test Rig Schematic.	20
14.	Facility Air Dryer.	21
15.	Combustor Test Rig Assembly Installed in Test Rig.	23
16.	Altitude-Relight Facility Air-Cooling System.	24
17.	Altitude-Relight Facility Fuel-Cooling System.	24
18.	Pressure-Atomizing Nozzle Results; Lightoff Characteristics for JP-4 Fuel.	31
19.	Pressure-Atomizing Nozzle Results; Lightoff Characteristics for Jet A Fuel.	32
20.	Pressure-Atomizing Nozzle Results; Lightoff Characteristics for Jet A + 2040 Solvent.	33

LIST OF ILLUSTRATIONS (Continued)

<u>Figure</u>		<u>Page</u>
21.	Pressure-Atomizing Nozzle Results; Lightoff Characteristics for No. 2 Diesel Fuel.	34
22.	Pressure-Atomizing Nozzle Results; Lightoff Characteristics for All Fuels Tested.	35
23.	Pressure-Atomizing Nozzle Results; Lightoff Correlation for All Fuels Tested.	36
24.	Pressure-Atomizing Nozzle Results; Full-Propagation Characteristics for JP-4 Fuel.	37
25.	Pressure-Atomizing Nozzle Results; Full-Propagation Characteristics for Jet A Fuel.	38
26.	Pressure-Atomizing Nozzle Results; Full-Propagation Characteristics for Jet A + 2040 Solvent.	39
27.	Pressure-Atomizing Nozzle Results; Full-Propagation Characteristics for No. 2 Diesel Fuel.	40
28.	Pressure-Atomizing Nozzle Results; Full-Propagation Characteristics for All Fuels Tested.	42
29.	Pressure-Atomizing Nozzle Results; Full-Propagation Correlation for All Fuels Tested.	43
30.	Pressure-Atomizing Nozzle Results; First-Cup-Blowout Characteristics for JP-4 Fuel.	44
31.	Pressure-Atomizing Nozzle Results; First-Cup-Blowout Characteristics for Jet A Fuel.	45
32.	Pressure-Atomizing Nozzle Results; First-Cup-Blowout Characteristics for Jet A + 2040 Solvent.	46
33.	Pressure-Atomizing Nozzle Results; First-Cup-Blowout Characteristics for No. 2 Diesel Fuel.	47
34.	Pressure-Atomizing Nozzle Results; First-Cup-Blowout Characteristics for All Fuels Tested.	48
35.	Pressure-Atomizing Nozzle Results; First-Cup-Blowout Correlation for All Fuels Tested.	49

LIST OF ILLUSTRATIONS (Concluded)

<u>Figure</u>		<u>Page</u>
36.	Pressure-Atomizing Nozzle Results; Complete-Blowout Characteristics for JP-4 Fuel.	50
37.	Pressure-Atomizing Nozzle Results; Complete-Blowout Characteristics for Jet A Fuel.	51
38.	Pressure-Atomizing Nozzle Results; Complete-Blowout Characteristics for Jet A + 2040 Solvent.	52
39.	Pressure-Atomizing Nozzle Results; Complete-Blowout Characteristics for No. 2 Diesel Fuel.	53
40.	Pressure-Atomizing Nozzle Results; Complete-Blowout Characteristics for All Fuels Tested.	54
41.	Pressure-Atomizing Nozzle Results; Complete-Blowout Correlation for All Fuels Tested.	55
42.	Lightoff Results for Air-Blast Nozzle.	57

LIST OF TABLES

<u>Table</u>		<u>Page</u>
1.	Fuel Analysis.	9
2.	Transfer Numbers and Quenching Parameters.	9
3.	Test Conditions for Pressure-Atomization Nozzles.	26
4.	Pressure-Atomizing Nozzle SMD Measurements (Jet A).	28
5.	Air-Blast Nozzles SMD Measurements, Effect of Fuel Flow Variation (Jet A).	28
6.	Air-Blast Nozzles SMD Measurements, Effect of Air Pressure Drop (Jet A).	29
7.	Air-Blast Nozzle SMD Measurements, Effect of Fuel Variation.	29
8.	Statistical Correlations for Pressure-Atomizing Nozzles.	30

1.0 SUMMARY

An experimental investigation of the effects of fuel properties on altitude-relight characteristics was conducted in a rectangular, five-swirl-cup, combustor sector at inlet air temperatures and flows representative of turbofan windmilling conditions. Four fuels having widely varying volatility properties (JF-4, Jet A, a blend of Jet A and 2040 Solvent, and No. 2 diesel) were used. The effects of fuel physical properties on atomization were eliminated by using four matched sets of pressure-atomizing nozzles designed to give a spray Sauter Mean Diameter (SMD) of $50 \pm 10 \mu\text{m}$ for each fuel at the same design fuel flow. A second series of tests was conducted with a single set of five prefilming, air-blast nozzles that were not designed to give a particular SMD spray.

Based on the test results, the following conclusions emerged:

- For comparable atomization levels (constant SMD), fuel volatility assumed only a secondary role for initial lightoff (first cup) and complete blowout. Initial lightoff and complete blowout were slightly poorer for fuels with decreased volatility.
- Full-propagation and first-cup-blowout characteristics were independent of fuel volatility and depended only on combustor operating conditions.
- The air-blast fuel nozzles had poorer ignition performance than the pressure-atomizing nozzles tested. Furthermore, the light-off results for air-blast nozzles showed a stronger effect due to volatility.

2.0 INTRODUCTION

Altitude-relight capability is one of the more important aircraft gas turbine combustion system parameters influenced by fuel-property variations. Several recent experimental and analytical studies have examined this aspect of performance in the context of more general investigation of fuel-property effects on aircraft engine combustion systems.

Typical of engine hardware-oriented experimental investigations were studies by Gleason, Oller, Shayeson, and Bahr on the J79 and F101 (References 1 and 2); Gleason et al. on smokeless J79 (Reference 3); Oller et al. on the J85 and TF39 (Reference 4); and Russel on the F100 and TF33 (Reference 5). In general, these studies were concerned with the effects of fuel properties on parameters such as gaseous emissions, smoke, flame radiation, combustor pattern factor, liner temperatures, ground start, and altitude relight. Fuel-property variations were found to have similar effects in all the various combustion systems. Hydrogen content was found to be a very good measure of fuel quality, and this parameter was used to correlate gaseous emissions, liner temperatures, flame radiation, pattern factor, and liner durability.

The nature of the foregoing programs was such that only the net effect of fuel variation was quantifiable for a given combustor parameter. For example, ignition characteristics were evaluated for different fuels using the same fuel injection system. Hence, the fuel physical properties such as viscosity, surface tension, and density, which govern the atomization process, were lumped together with other properties such as volatility and aromatic content.

Reference 6 describes a study which sought to separate the effect of physical and chemical properties on combustion parameters. A highly atomized spray was used to minimize physical-property effects in a cylindrical burner. Hydrogen and naphthalene contents were found to be significant determinants of fuel effects on radiation, liner temperatures, and smoke. Furthermore, smoke point, which is a fuel specification parameter, was found to be an adequate global indicator of fuel chemical-property effects.

In order to design future generations of fuel-flexible combustors, it is essential to consider each performance parameter and isolate fuel effects into groups or categories that can be studied in detail to guide design methodology. This program, conducted by the GE Aircraft Engine Business Group under contract to the NASA Lewis Research Center, represents such an attempt.

The major objective of this program was to evaluate fuel-property effects on altitude-relight and blowout characteristics by isolating atomization effects from volatility effects. Four fuels with widely varying volatility characteristics (JP-4, Jet A, a blend of Jet A and 2040 Solvent, and Diesel 2) were selected as the test fuels. The fuel physical-property effects on atomization were eliminated by maintaining the same SMD for all four fuels at the same design fuel flow rate.

A five-swirl-cup, rectangular, two-dimensional (2D) combustor featuring engine-type swirlers but simple, bolt-on liner construction was designed and fabricated. The combustor geometry was dictated by the original requirement of the program to be able to accommodate geometry modifications, flow-split variations, and subscale combustor hardware in the same rig. As a result of budget constraints, the program scope was changed to exclude the subscale hardware design. The simplicity of the design, however, retains the option to incorporate modifications if desired at a future date.

Two types of fuel nozzles were used. The first was a pressure-atomizing, simplex design. For each of the four fuels, a matched set of five fuel nozzles was obtained. The atomization criterion was to produce a spray with an SMD of $50 \pm 10 \mu\text{m}$ at 256 K (0°F) and 0.1 MPa (1 atm) for each fuel and nozzle set. Extensive spray tests conducted with Jet A in the spray-characterization facility indicated that the criterion of fine atomization (that is, SMD of $50 \pm 10 \mu\text{m}$) was met.

The second type of fuel injector was a prefilming, air-blast design. The same set of five air-blast nozzles was used for all four fuels. There was no SMD criterion for the air-blast nozzles for this task. Since the same nozzles were used for all four fuels, the effects of fuel physical properties on atomization were expected to be reflected in lightoff and blowout characteristics in addition to fuel volatility effects. Also, it is usually necessary to tailor airflow splits closely between the air-blast nozzles and the swirlers since the air-blast nozzle forms part of the aerodynamic path of the dome and contributes to the primary-zone stoichiometry. However, development of a swirler in conjunction with the prefilming air-blast nozzles was outside the scope of this program, and the air-blast nozzles were run with the same dome hardware as the pressure-atomizing nozzles.

The altitude relight map of the reference engine (CF6-80A), giving the relight envelope in terms of pressure altitude and flight Mach number, is shown in Figures 1 and 2. For clarity, the engine combustor airflows and inlet total pressures are indicated in Figure 1, and the corresponding inlet temperatures are shown in Figure 2. The combustor airflows, pressures, and temperatures were derived from the windmilling characteristics of the reference engine. For this program, four operating combustor inlet temperatures (239 K, 250 K, 261 K, and 272 K) were selected to cover a wide range of test conditions. These nominal points are shown in Figure 1.

From the altitude-relight map of the reference engine, the baseline airflows (corresponding to windmilling conditions) at the four nominal test points were determined. Two additional airflows at each temperature were included to cover a $\pm 25\%$ variation about the baseline airflows. Fuel flow for all the test conditions was kept constant at 11.6 g/s, corresponding to the minimum fuel flow schedule of the reference engine.

While the use of engine swirlers and a five-swirl-cup sector rig was a significant step toward representing engine combustor hardware, it must be emphasized that a 2D combustor of the type used here does not faithfully replicate the combustion and ignition characteristics of a full-annular engine

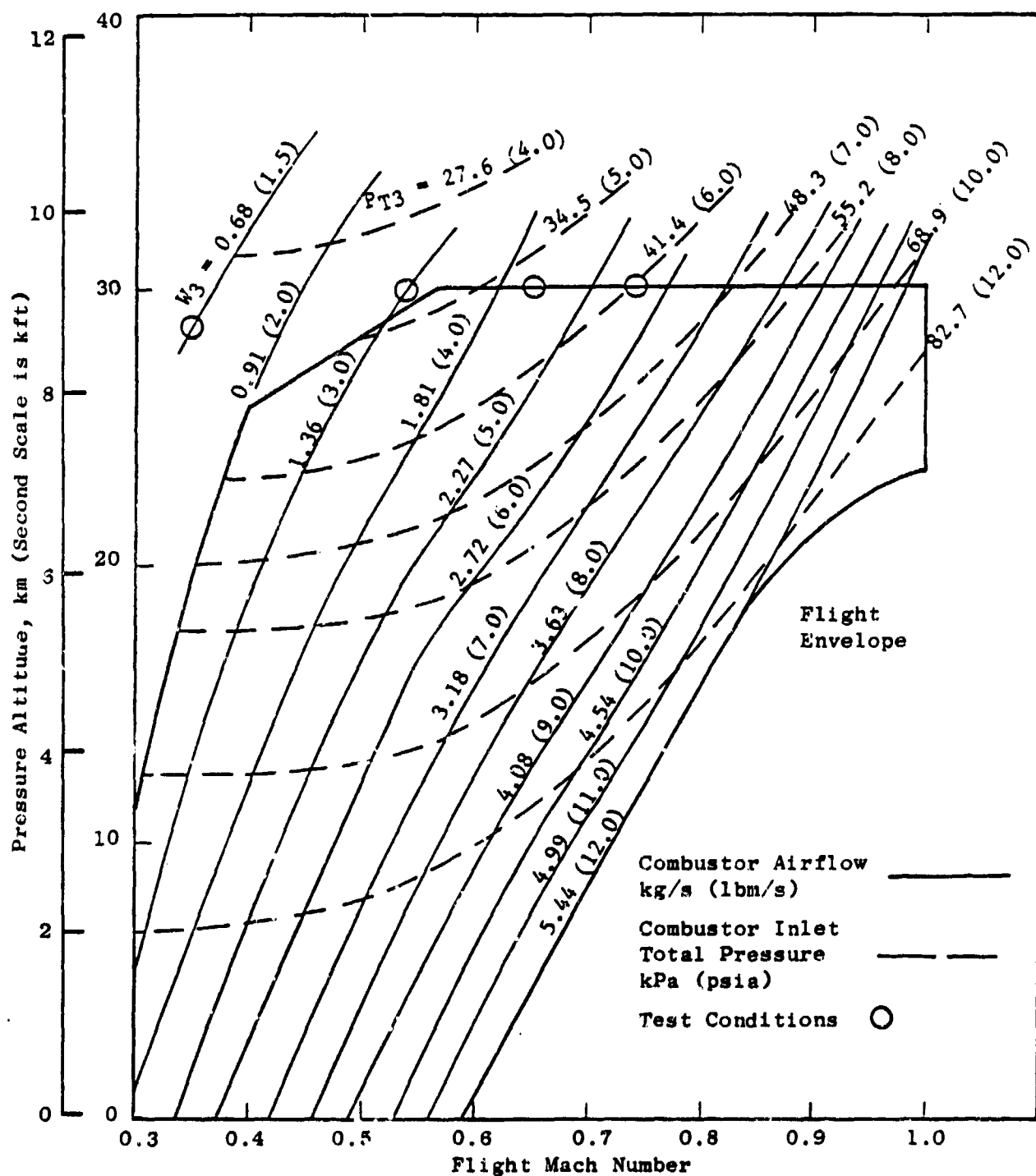


Figure 1. Reference Engine Altitude Relight Map; Combustor Airflows and Inlet Pressures Under Windmilling Conditions.

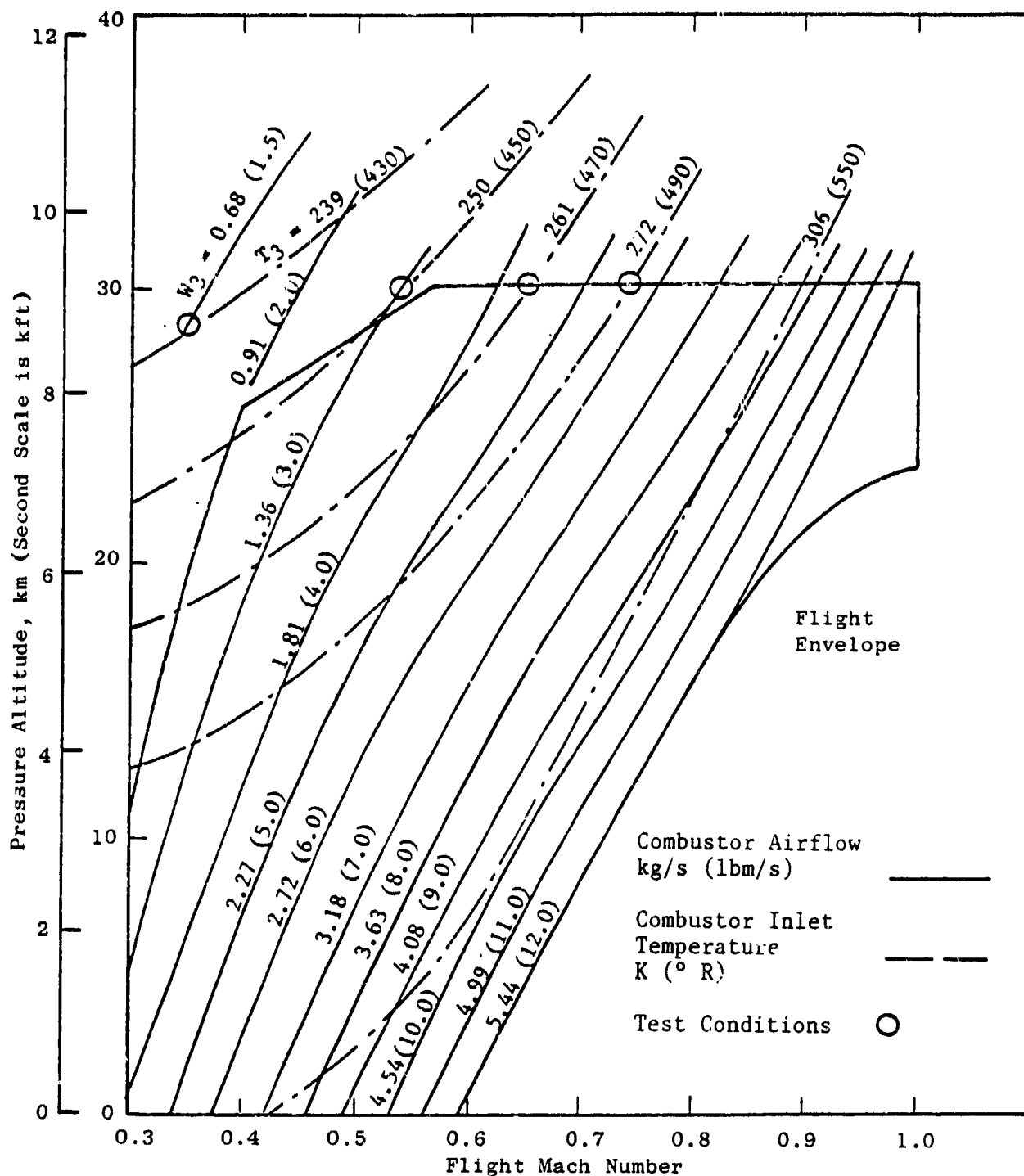


Figure 2. Reference Engine Altitude Relight Map; Combustor Airflows and Inlet Temperatures Under Windmilling Conditions.

combustor because the flow fields are dissimilar. However, the 2D combustor fulfilled the intended objective of providing a vehicle for comparing the altitude-ignition characteristics of different fuels under inlet conditions typical of an aircraft gas turbine combustor while retaining the flexibility to accommodate future combustor geometry modifications.

3.0 TEST FUELS AND FUEL NOZZLES

3.1 TEST FUELS

The ignition characteristics of gas turbine combustion systems are significantly affected by fuel properties that may be classified under two major groups: properties influencing ignition through effect on the atomization quality of the fuel spray and those influencing ignition through effect on the evaporation rate of the droplets which, in turn, governs gas-phase stoichiometry in the ignition zone.

Fuel properties controlling atomization quality for a given combustor/fuel nozzle system are viscosity, surface tension, and density. This dependence is in accord with the classic description of atomization consisting of formation of initial surface disturbances in the fuel jet, formation of ligaments of fuel that break into large drops, and further shattering of the large drops into smaller droplets. Viscosity represents internal fuel resistance to velocity gradients in the liquid phase - which are essential ingredients of the atomization process. Surface tension also tends to oppose the atomization process which, in essence, seeks to increase the total free-surface area of the droplets. Density enters the picture through inertia force that provides the driving mechanism for atomization. The typical way to characterize the quality of atomization in a given spray is to relate to the SMD which, by definition, is the diameter of an equivalent droplet that has the same volume-to-surface-area ratio as the entire ensemble of droplets in the spray.

Fuel volatility affects the evaporation of the droplets and hence the production of an ignitable fuel vapor/air mixture in the ignition zone and may be characterized by the distillation range, vapor pressure, flash point, or mass transfer number (B). Often, distillation characteristics are specified by the 10% boiling point or by the 50% boiling point in the ASTM distillation curve. Vapor pressure is defined as the pressure exerted by vapor in equilibrium with the liquid at a given temperature in the absence of air. Unlike pure substances, the vapor pressure of liquid hydrocarbon fuels such as the ones under consideration here decreases with the amount vaporized; this is due to the change in composition as the lighter fractions vaporize first followed by progressively heavier fractions. Hence, for such fuels, the "true" vapor pressure is defined in the limit of the vapor-to-liquid ratio approaching zero. For example, at a given temperature, JP-4, which is more volatile, has a higher true vapor pressure than Diesel 2, the least volatile fuel considered in this program.

The mass transfer number (B), sometimes referred to as the Spalding transfer number, is defined in Reference 7 as:

$$B = \frac{C_g (T_\infty - T_B)}{L + C_l (T_B - T_i)}$$

where: C_g is the average gas-phase specific heat,
 T_B is temperature at the droplet surface,
 L is the latent heat of vaporization of the fuel,
 C_l is the specific heat of fuel (liquid),
 T_∞ is the far-field gas temperature,
and T_i is the initial temperature of the fuel droplet. .

The transfer number B is a significant fuel parameter for ignition considerations of spray combustion systems because it expresses the basic balance between the thermal energy required to raise the droplet temperature to the boiling point and vaporize it and the thermal energy available in the spark kernel. In order to maintain the mathematics at a tractable level, droplet-evaporation theories introduce simplifications such as single-component fuel (unlike typical hydrocarbon liquid fuels such as considered here), spherical symmetry, neglect of radiation heat transfer from the spark kernel (or flame zone for a burning droplet), unity Lewis number, etc. The transfer number B is widely employed in modern theoretical treatments of ignition and blowout phenomena (References 8, 9, and 10) in a gas turbine combustor environment. The transfer number B is made use of in the definition of the "quenching distance" as an ignition criterion (Reference 8). The quenching distance may be viewed as the limiting size of the spark kernel for which heat generated inside the incipient kernel just balances the heat loss by conduction and turbulent diffusion:

$$d_q = [\rho_{\text{fuel}}^{\text{SMD}} / \rho_{\text{air}} \phi \ln(1+B)]^{0.5}$$

where: d_q = quenching distance,
 ϕ = equivalent ratio,
 ρ_{fuel} = fuel density,
and ρ_{air} = air density.

A similar expression occurs in the theoretical approach to blowout by Ballal and Lefebvre (Reference 11). For evaluating fuel-volatility effects with the same SMD for all the fuels, it is sufficient to consider the group $\rho_{\text{fuel}} / \ln(1+B)$. By using the specific gravity ρ_s instead of the density, the group could be rendered nondimensional. For convenience, it is referred to as the "quenching parameter." It is important to note that the term B occurs only in the form of $\ln(1+B)$ in the analysis; hence, a large change in B results in a smaller change in the evaporation rate of a droplet.

Table 1 lists the results of analyses of the four test fuels. It is seen that, based on the 10% boiling point or the 50% boiling point, JP-4 is the most volatile of the four and Diesel 2 is the least volatile. Table 2 lists

Table 1. Fuel Analysis.

	<u>JP-4</u>	<u>Jet A</u>	<u>Jet A + 2040 Solvent</u>	<u>No. 2 Diesel</u>
Specific Gravity	0.7568	0.819	0.8366	0.8498
Flash Point (K)	---	326	335	333
Freezing Point (K)	<211	225	223	* 250
Smoke Point (mm)	32	24	16	15.5
Net Heat of Combustion (MJ/kg)	43.72	43.03	42.58	42.65
Viscosity (cSt) at 253 K	1.8	6.2	5.6	16.5
at 293 K	0.96	2.2	2.06	4.1
at 311 K	0.78	1.62	1.56	2.79
Surface Tension (dyne/cm) at 298 K	22.8	26.6	27.2	28.4
Hydrogen (Weight %)	14.49	13.75	12.75	12.95
Total Sulfur (Weight %)	<0.01	<0.01	0.024	0.019
Aromatics (Weight %)	11.8	18.6	31.6	---
Olefins (Weight %)	0.9	0.9	0.8	---
Saturates (Weight %)	87.3	80.5	67.6	---
Boiling Point (K), Initial	360	440	450	450
10%	365	467	471	487
20%	377	475	477	502
30%	386	482	481	513
50%	417	491	491	528
70%	456	502	---	560
90%	497	514	520	596
95%	510	524	530	596
End	527	536	540	618
Vapor Pressure (kPa) at 311 K	19.5	2.8	3.3	2.7

* Pour Point

Table 2. Transfer Numbers and Quenching Parameters.

<u>Fuel</u>	<u>Transfer Number, B</u>	<u>Quenching Parameter, $\rho_s / \ln(1+B)$</u>
JP-4	6.1	0.3861
Jet A	3.75	0.5256
Jet A + 3040 Solvent	3.71	0.5484
No. 2 Diesel	2.8	0.6366

the transfer numbers and the group quenching parameters for the four fuels under consideration here. As before, JP-4 is the most volatile (highest evaporation rate for a given initial droplet size) and Diesel 2 is the least volatile of the fuels.

3.2 FUEL NOZZLES

Two types of fuel nozzles were employed in this investigation: pressure-atomizing simplex nozzles and prefilming air-blast nozzles.

3.2.1 Pressure-Atomizing Nozzles

The basic requirement of the program was to separate atomization and volatility effects relative to altitude relight and blowout characteristics. For the pressure-atomizing nozzles, the atomization criterion was $50 \pm 10 \mu\text{m}$ SMD at 256 K (0°F) and 0.1 MPa (1 atm) for all four fuels at the same design fuel flow. Four sets of ten simplex fuel nozzle tips designed according to the above SMD criterion were obtained and tested. The flow number for each nozzle/fuel combination was selected to give the required SMD ($50 \pm 10 \mu\text{m}$) at the design fuel flow. A matched set of five nozzles was selected for each of the four fuels based on the fuel nozzle calibrations and visual evaluation of fuel spray.

Figure 3 shows the tip details of the simplex pressure-atomizing nozzles. The pressure-atomizing fuel nozzle holder is illustrated in Figure 4. A copper-constantan thermocouple was inserted in each of the five fuel-nozzle stems to measure the local fuel temperature. Prior to each fuel change during altitude-relight testing, the corresponding pressure-atomizing nozzle tips were installed and aligned in the combustor.

3.2.2 Prefilming Air-Blast Nozzles

The prefilming air blast nozzles have an attractive feature in the use of available combustor pressure drop to accomplish atomization; they do not need high fuel injection pressures. Unlike the pressure-atomizing nozzles, an atomization criterion was not specified for the air-blast nozzles since the cost of obtaining air-blast nozzles specially designed for each fuel for a given SMD would have been prohibitive for this program. Thus, one set of air-blast nozzles was used for all four fuels. In addition to volatility effects, some atomization effects were therefore expected to be reflected in altitude relight and blowout characteristics. Furthermore, since the air-blast nozzles are an integral part of the combustor aerodynamic path contributing to the primary-zone stoichiometry, it is usually necessary to optimize the flow split between the combustor dome and the air-blast nozzle. However, development of the dome in conjunction with the air-blast nozzles was beyond the scope of this program. The single set of five prefilming air-blast nozzles were therefore run with the same dome hardware as the pressure-atomizing nozzles.

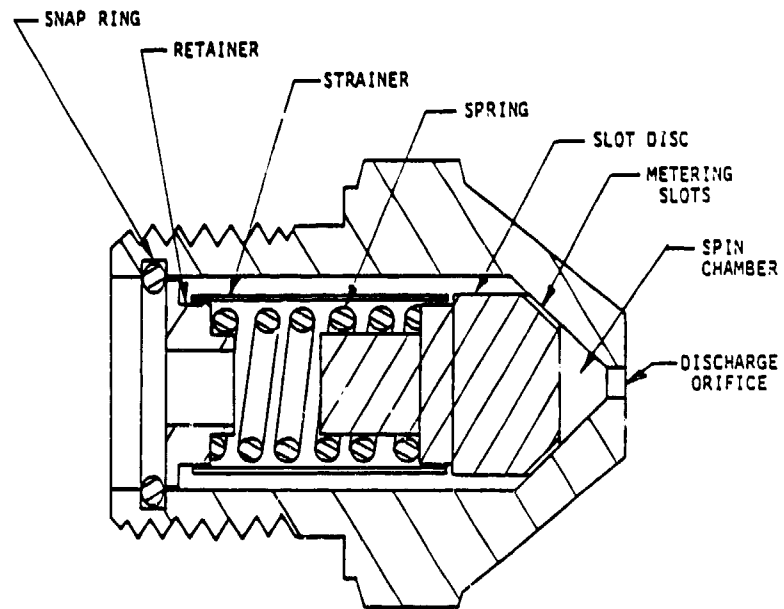


Figure 3. Pressure-Atomizing Nozzle.

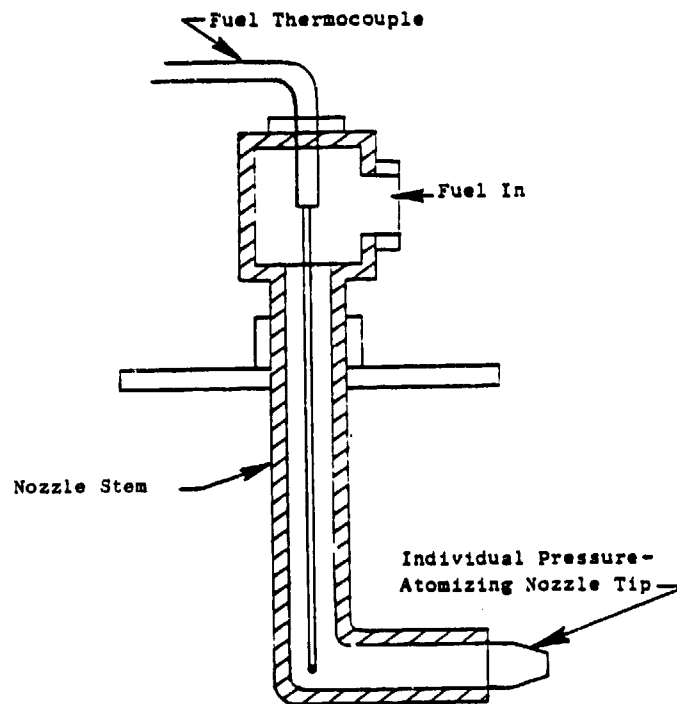


Figure 4. Test Combustor Fuel Injector Schematic.

Figure 5 is a cross-sectional view of the prefilming air-blast nozzle. The air-blast action is enhanced by subjecting the fuel film to air streams on both sides. Figure 6 shows two photographs of the nozzle; the swirl vanes in the inner passage and the slots in the outer passage can be seen.

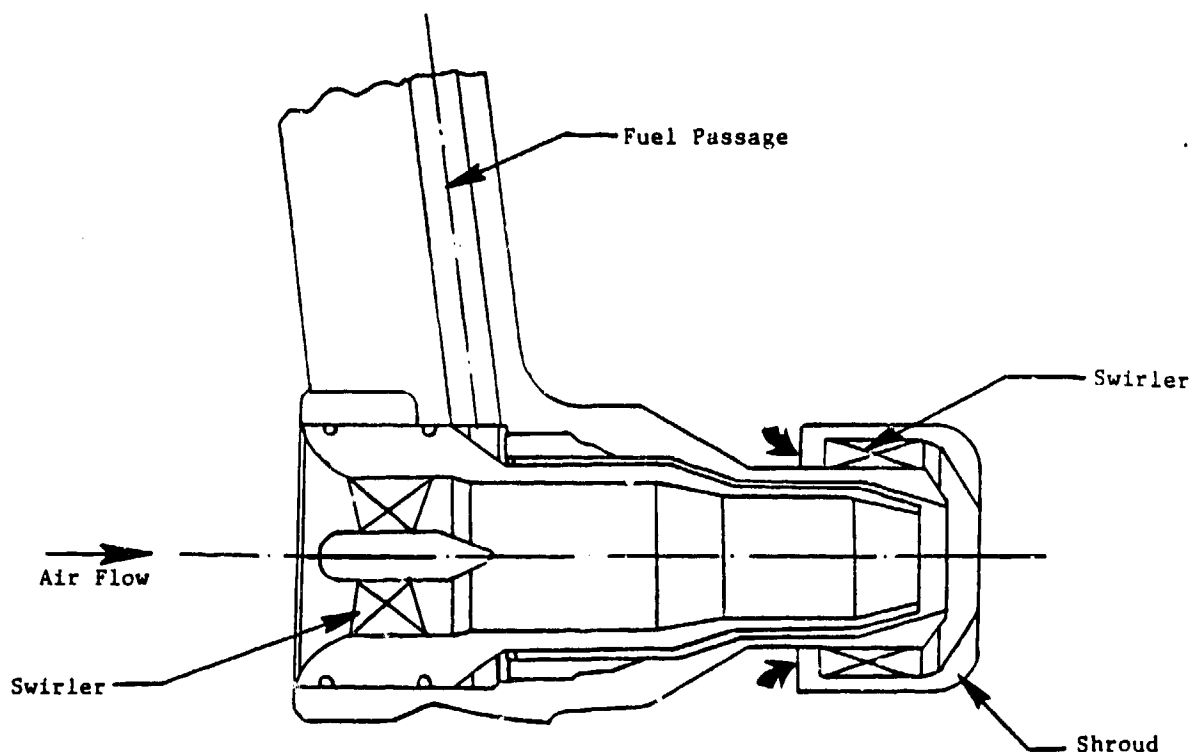


Figure 5. Air-Blast Fuel Nozzle, Tip Details.

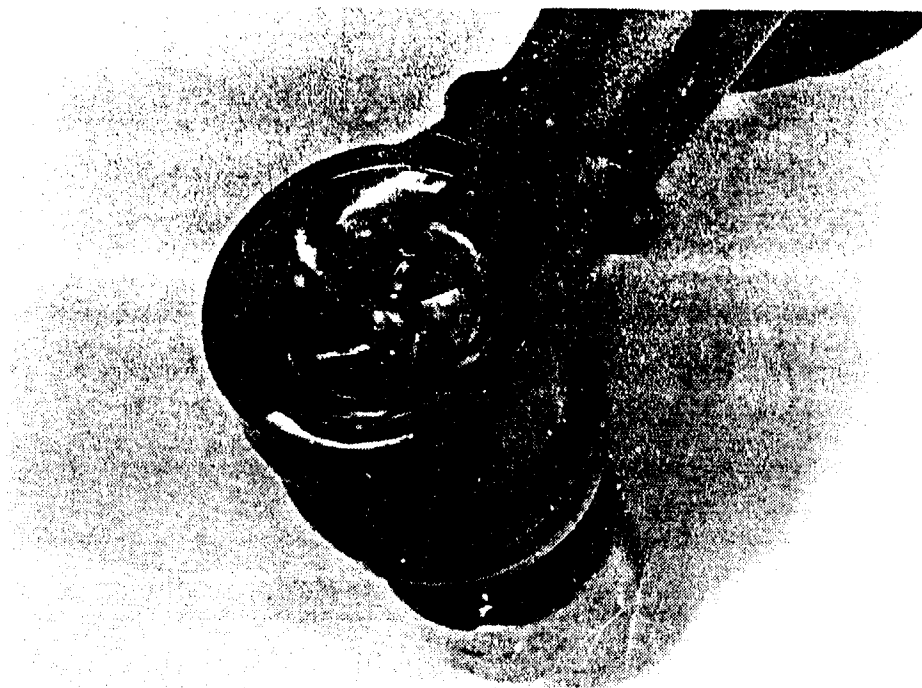
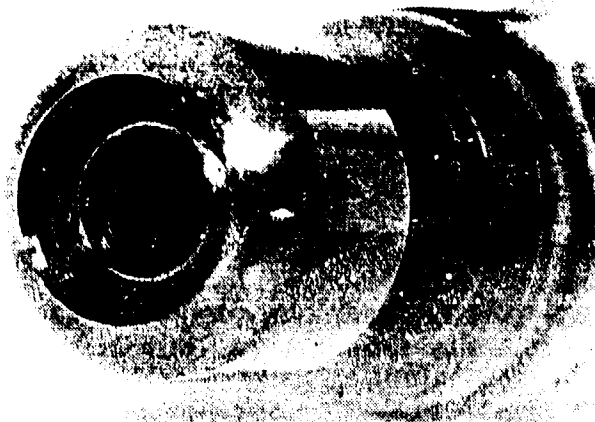


Figure 6. Photographs of Air-Blast Fuel Nozzle.

4.0 TEST FACILITIES

4.1 DROPLET-MEASUREMENT FACILITY

The measurements were conducted in the Advanced Combustion Laboratories Droplet Measurement Facility which features a droplet-sizing interferometer manufactured by Spectron Development Laboratories, Inc.

The droplet-sizing interferometer is a device that uses scattered light from droplets or solid particles to define size and velocity distributions. Figure 7 is a schematic of the instrument. The transmitter unit of the optics package includes a 25-mW helium-neon laser, beam-steering devices, a beam expander, beam splitter, and rotating and focussing components. The receiver unit consists of the receiving or collection optics, photomultiplier tube assembly, and high-voltage power supply. In the system used in this program, the collection unit is at right angles to the incident beam. The fuel spray is oriented vertically downwards.

The principle of operation of the instrument is illustrated in Figure 8. The laser beam is split into two beams of nearly equal intensity that are then made to intersect by the system beam splitter. The region of intersection is referred to as the probe volume. It is at this spatial volume or "point" that the droplet measurements are made. The probe volume is shown in Figure 8. The intersection of the two coherent laser beams forms interference fringes that comprise alternating bright and dark zones. Droplets passing through the probe volume scatter light of higher intensity when in the middle of a bright fringe. A photodetector receiving this scattered light superimposes an output signal on it. This signal is processed by the electronics package to yield both droplet size and velocity information. The procedure for computing the overall SMD of the spray from measurements made at several positions along a diameter in a plane normal to the spray axis is described in Section 5 - Test Procedures.

4.2 TEST COMBUSTOR

Figure 9 is a cross section of the rectangular, five-swirl-cup, test combustor. The swirler assemblies consisted of counterrotating primary and secondary swirlers that produced a zone of intense shear. The dome was flat, and the distance between the top and bottom liner was kept constant for the entire length of the combustor. The liners were made of several sheet metal plates bolted together for ease of disassembly. Although the requirement to accommodate several geometry variants was dropped during the course of the program, the simple-assembly feature was retained so that the option to change the combustor geometry could be exercised in future experiments.

Each panel of the liners (six inner and six outer) was cooled by a slot fed by a series of 91 cooling holes spanning the width of the combustor. The combustor dome height as defined in the figure was 121 mm, and the overall

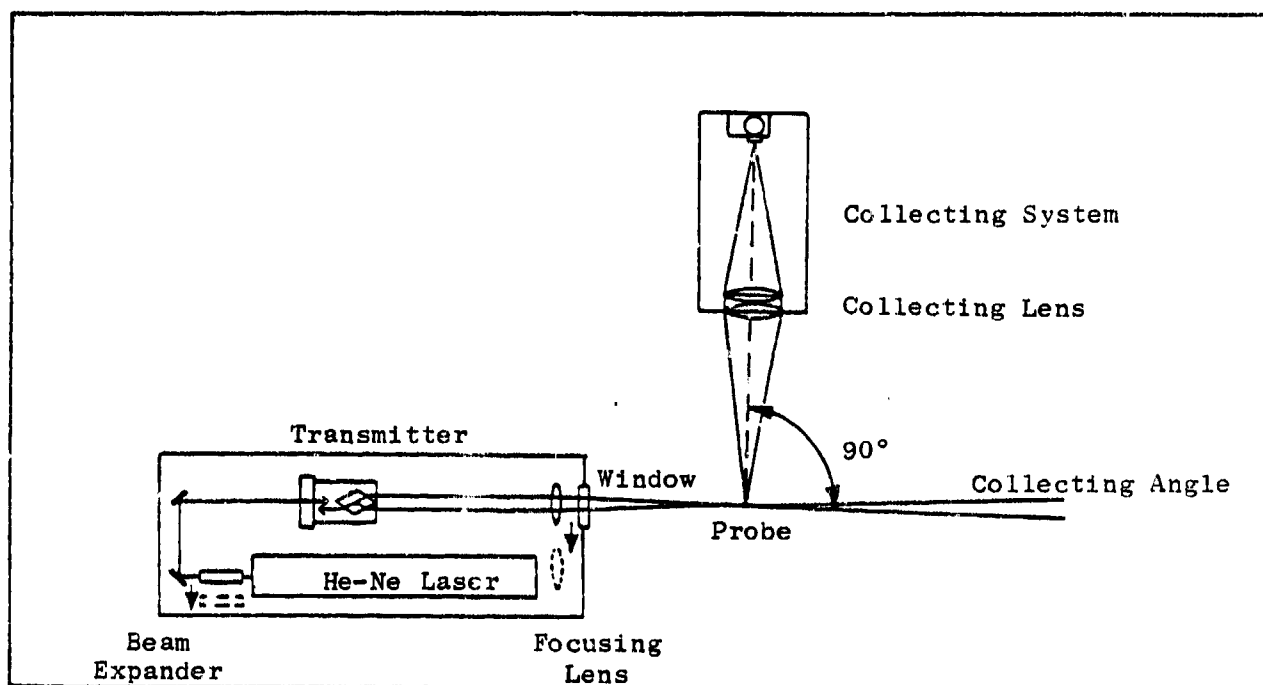


Figure 7. Spectron Droplet-Sizing Interferometer.

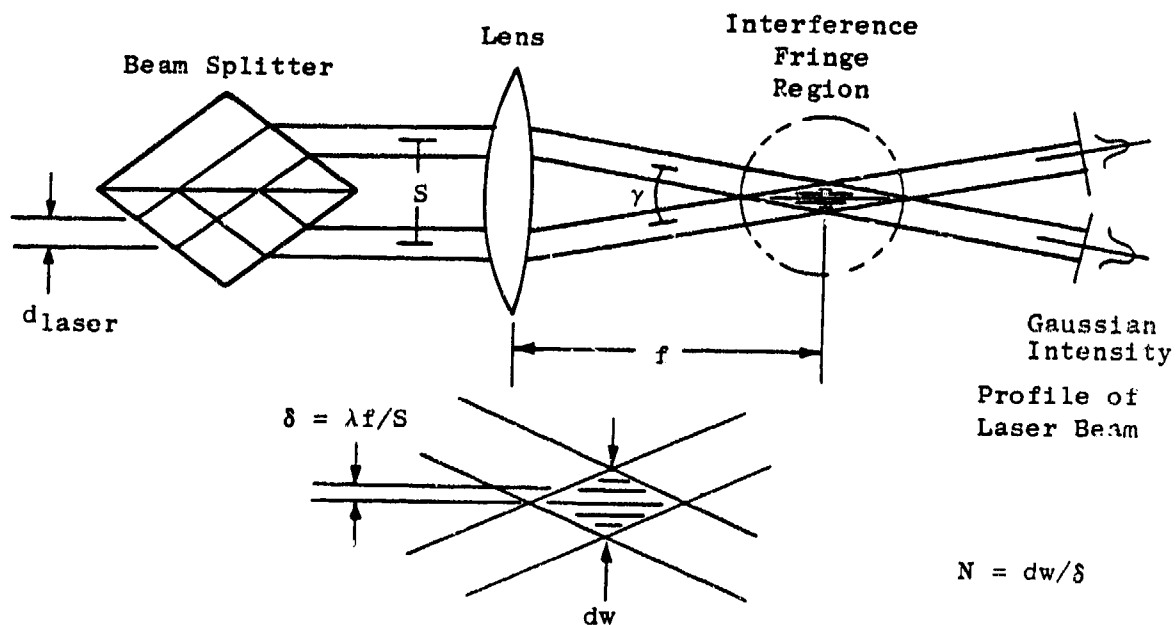


Figure 8. Spectron Droplet-Sizing Interferometer Operating Principle.

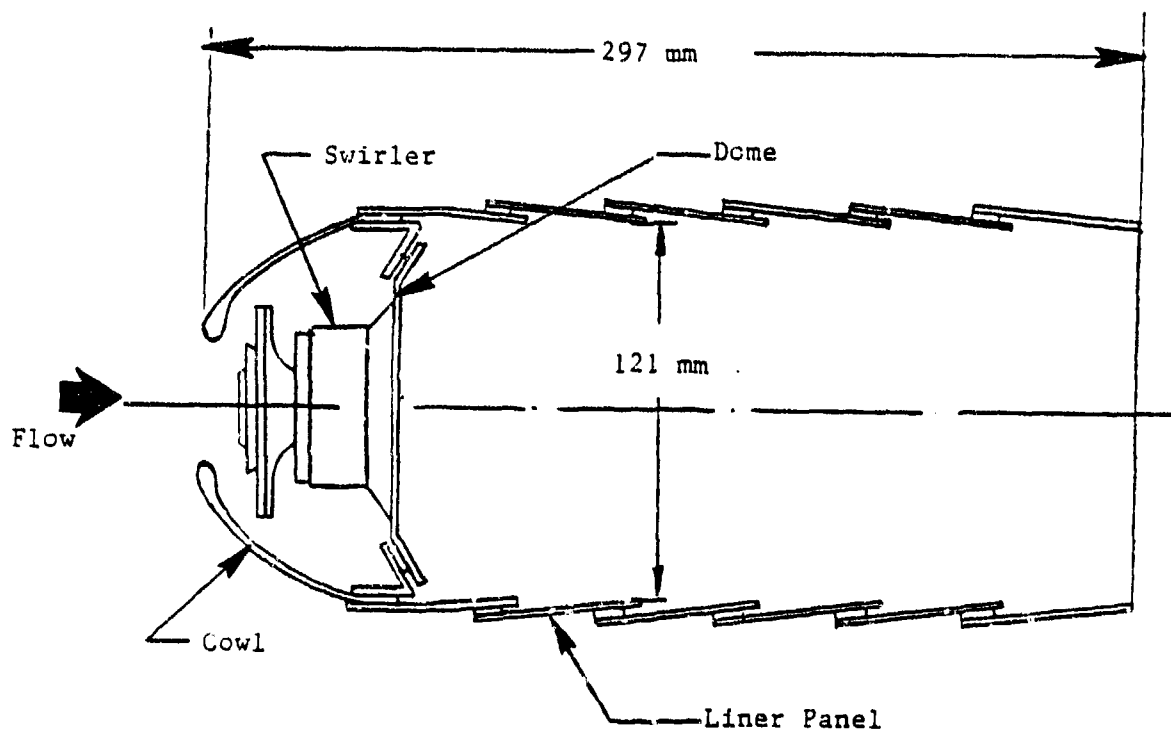


Figure 9. Schematic of the Combustor.

length of the combustor was 297 mm. The combustor width was 343.8 mm; this included five swirl cups and represented a 60° sector of the reference-engine combustor. Figure 10 is a close-up of the dome region viewed from downstream; the swirler passages can be seen. The combustor liner assembly, Figure 11, indicates the layout of the cooling-slot feeder holes and the dilution holes in the panels. Figure 12 is a front view of the dome.

4.3 ALTITUDE-RELIGHT RIG

Figure 13 is a schematic of the altitude-relight facility in which the test program was conducted. Air from the facility compressed air supply enters an air dryer that is capable of drying 1 kg/s of air to 233 K dew point and provides 12 hours continuous operation at that airflow. Figure 14 shows the air dryer located outside the test cell. The dry air passes through an air/liquid nitrogen heat exchanger where it is cooled to the required inlet temperature conditions as monitored by the inlet thermocouples. The cold air then enters a plenum that provides uniform inlet flow. The combustor is housed in a combustor casing section that includes provision for mounting the fuel injectors, inlet instrumentation, and ignitor. The instrumentation spool immediately following the combustor section contains five Type K thermocouples in line with the fuel injector centerline to detect ignition. The gas stream

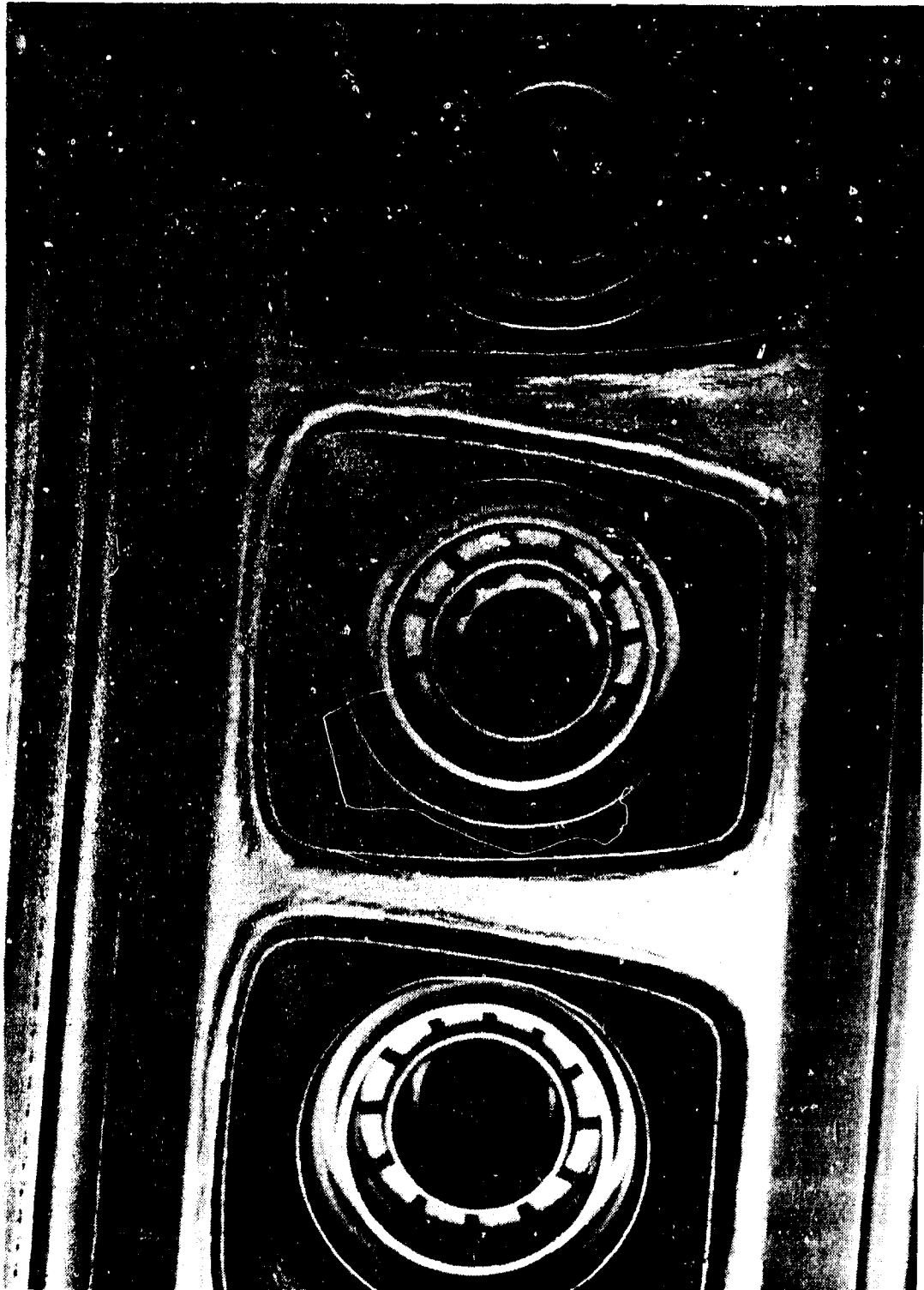


Figure 10. Photo of Sector Combustor Looking Forward Into Dome.

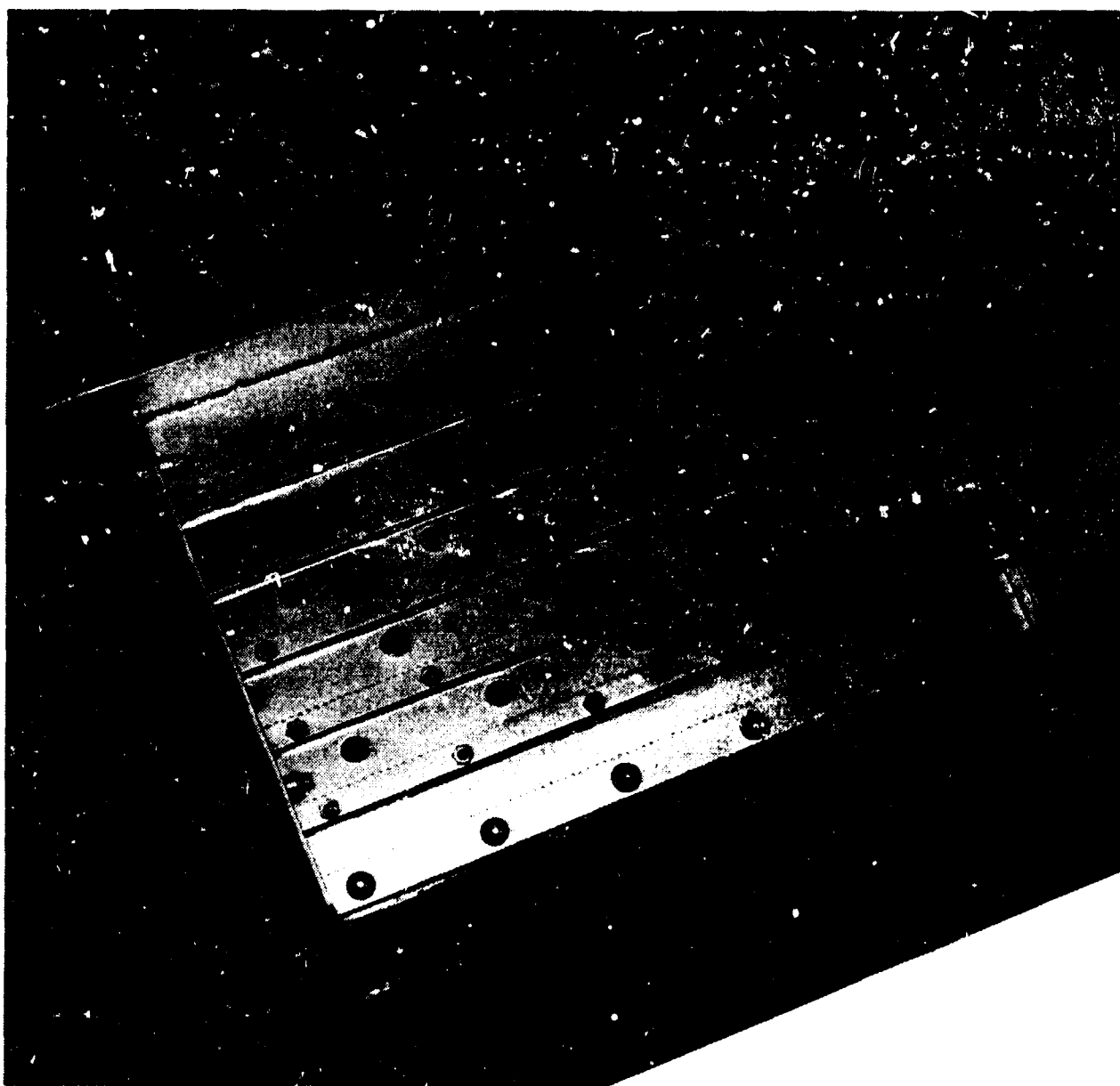


Figure 11. Sector Combustor Assembly.

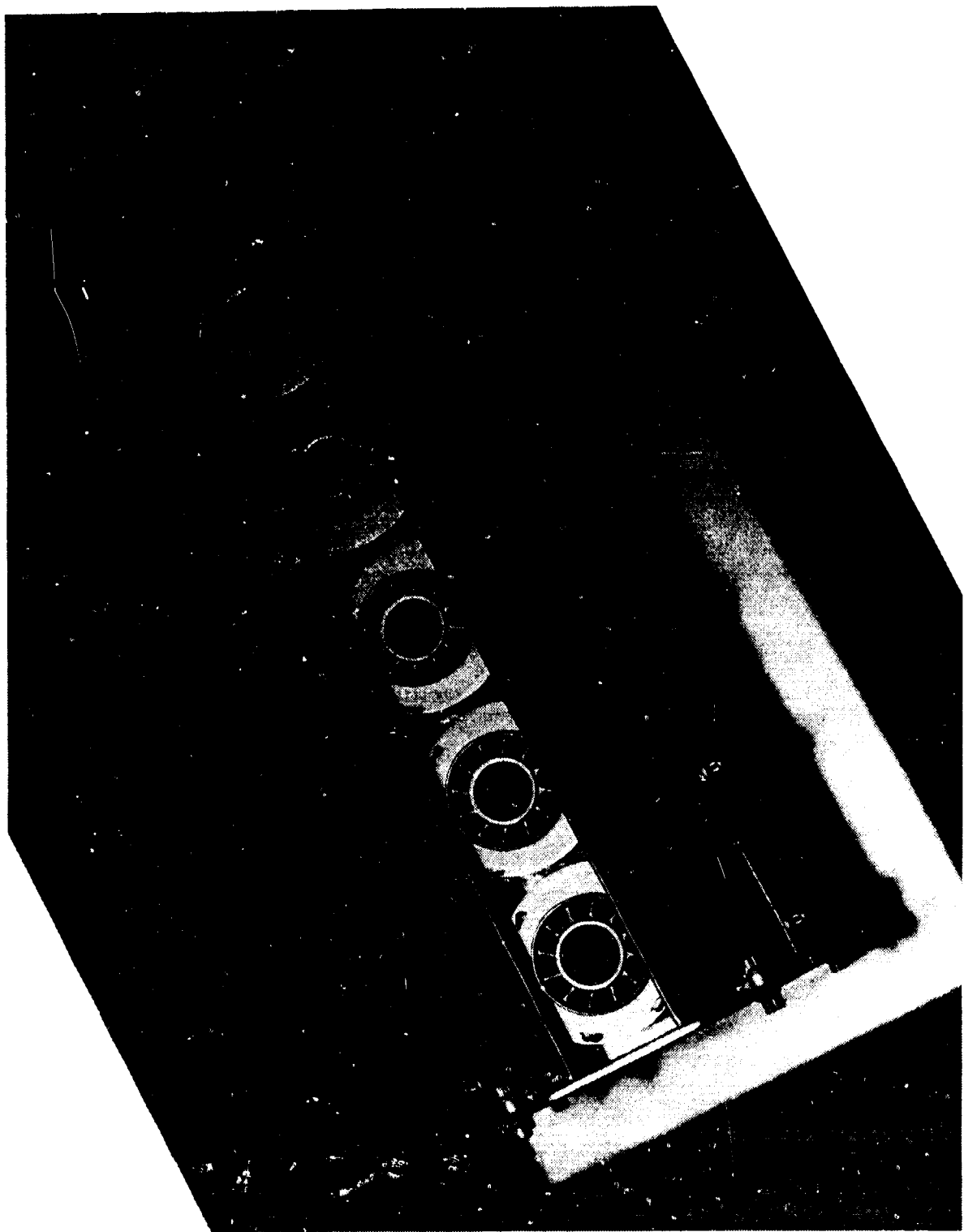


Figure 12. Front View of Dome.

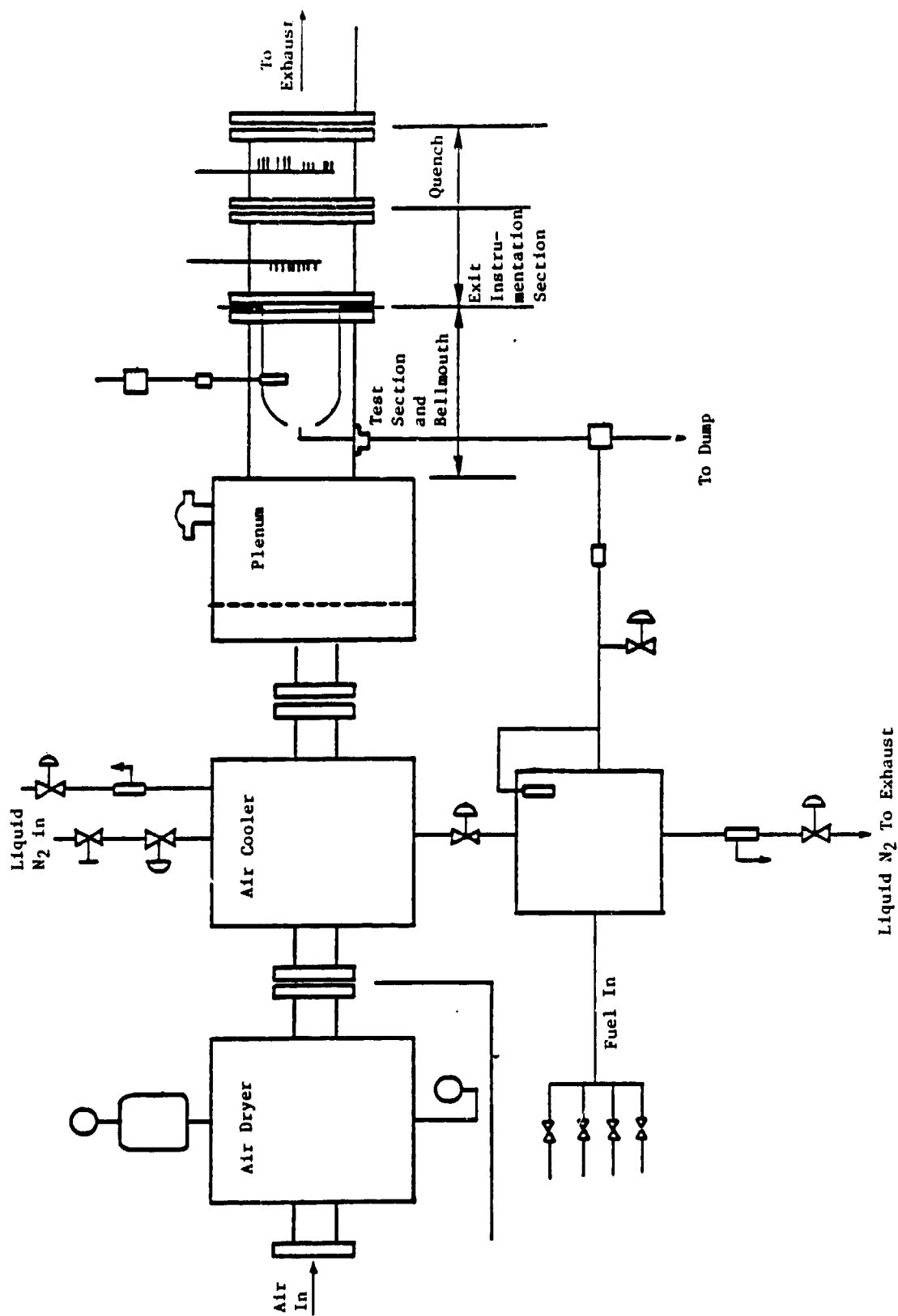


Figure 13. Altitude-Relight Test Rig Schematic.

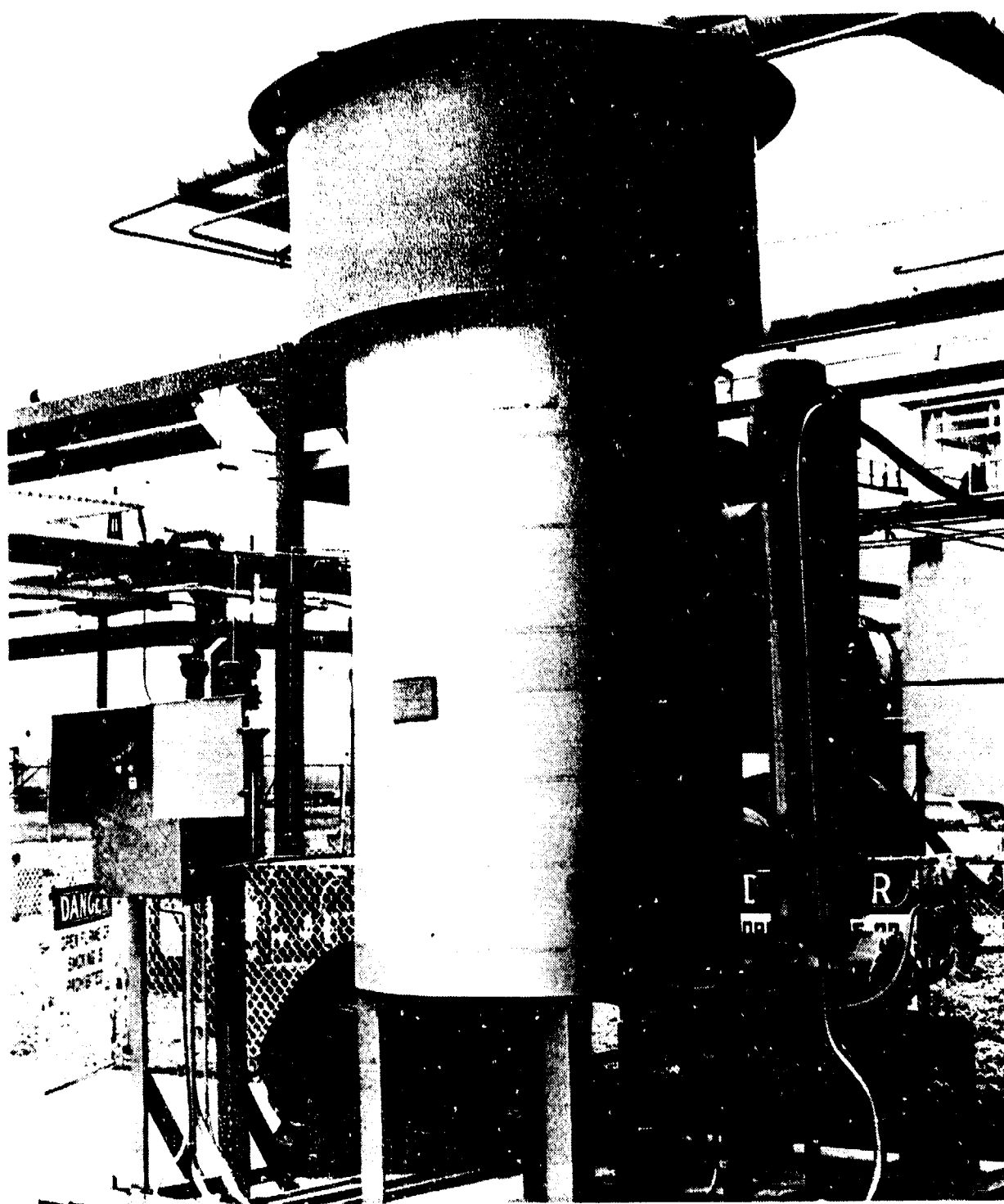


Figure 14. Facility Air Dryer.

is water-quenched and exhausted via a steam ejector that provides the vacuum for simulated altitude conditions.

Figure 15 is a view of the combustor casing showing the inlet total pressure instrumentation, inlet thermocouples, fuel injector mounting pads, and the ignitor. At the inlet, there are four 3-element total pressure rakes. Five copper-constantan thermocouples in line with the swirler centerlines and five copper-constantan thermocouples in the fuel-nozzle stems monitor the inlet air and fuel temperatures, respectively. In addition to the five Type K thermocouples in the instrumentation spool, five additional Type K thermocouples in line with the swirlers in the primary zone are used to detect lightoff and blowout. The latter thermocouples mitigate the potential for ambiguities due to swirl and crossflow effects. The ignition system delivered two sparks per second at an energy level of two joules.

4.3.1 Air-Cooling System

The air-cooling system is shown schematically in Figure 16. A control valve regulates liquid nitrogen flow from a tank to the coil side of a compact heat exchanger. A relief valve and a backpressure-control valve on the downstream side provide safety relief and fine control. Dry air enters the shell side of the heat exchanger and exits to the test rig plenum. The system operated satisfactorily throughout the test program.

4.3.2 Fuel Cooling System

Figure 17 is a schematic of the fuel-cooling system. Nitrogen control is virtually identical to that on the air-cooling system. The heat exchanger consists of an alcohol bath with separate coils for liquid nitrogen and fuel. A pneumatically operated stirrer provides mixing in the alcohol bath. The fuel system incorporates on/off solenoid valves, flow control valves, and a calibrated turbine flowmeter.

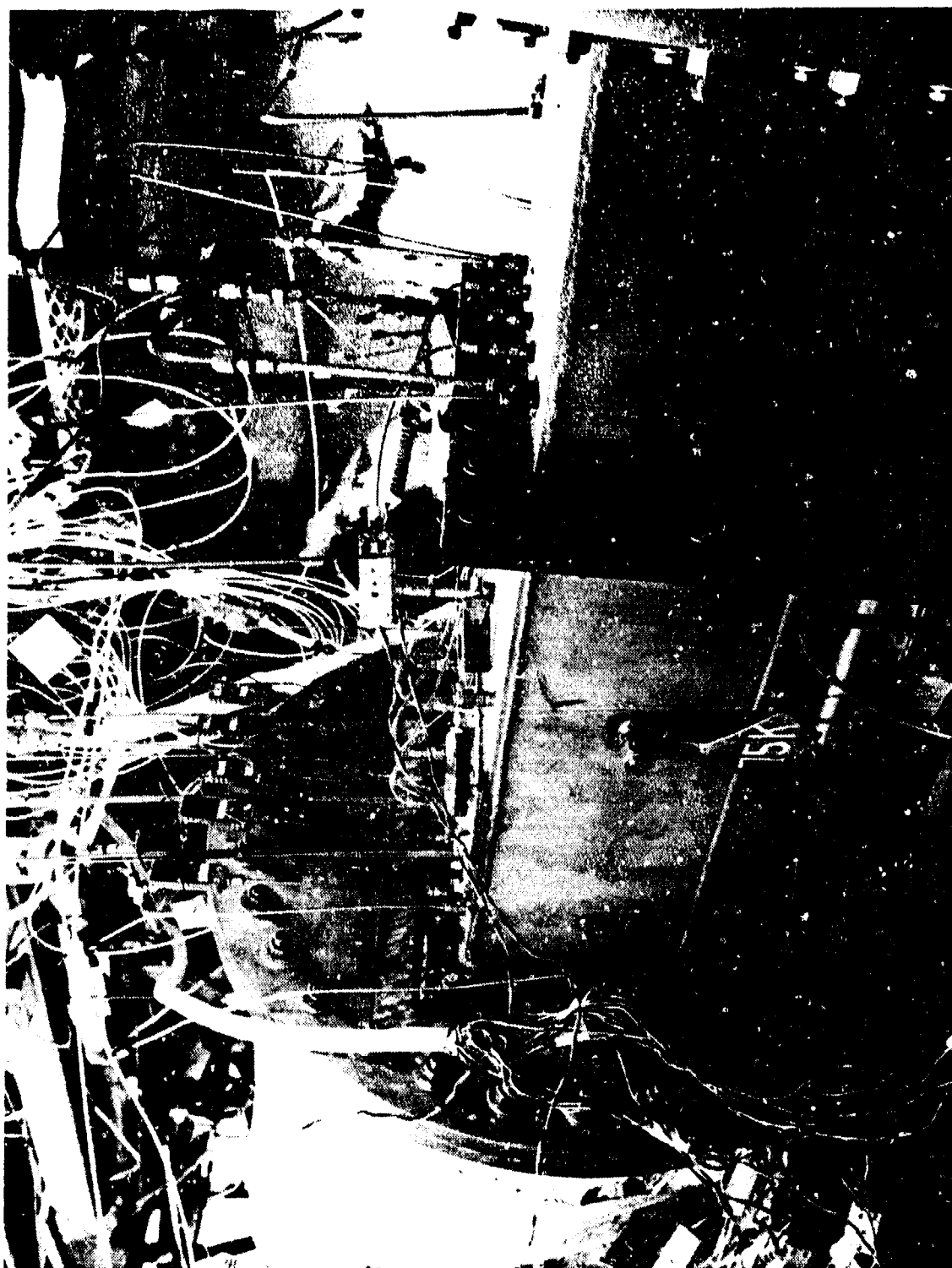


Figure 15. Combustor Test Rig Assembly Installed in Test Rig.

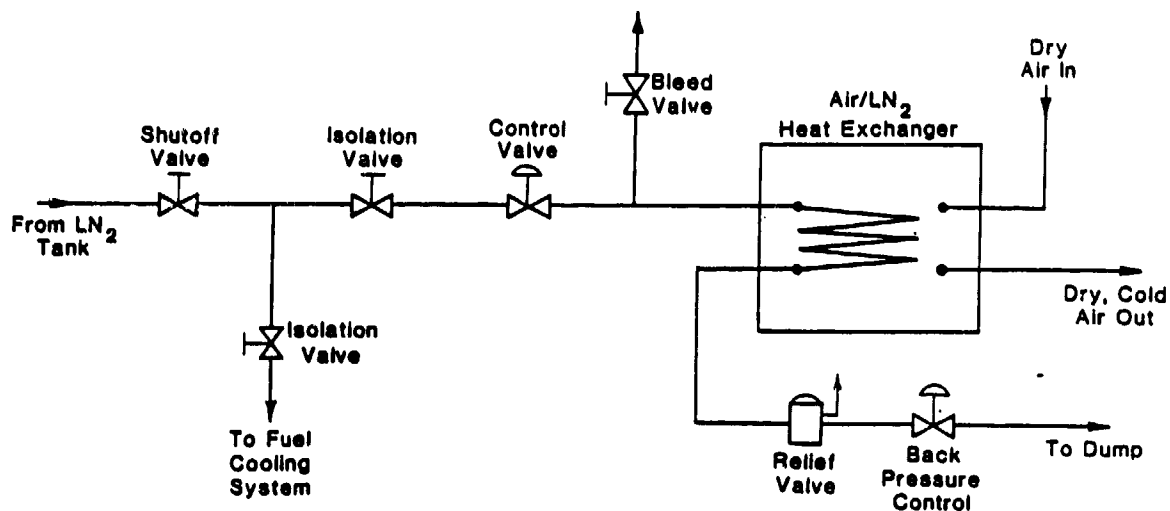


Figure 16. Altitude-Relight Facility Air-Cooling System.

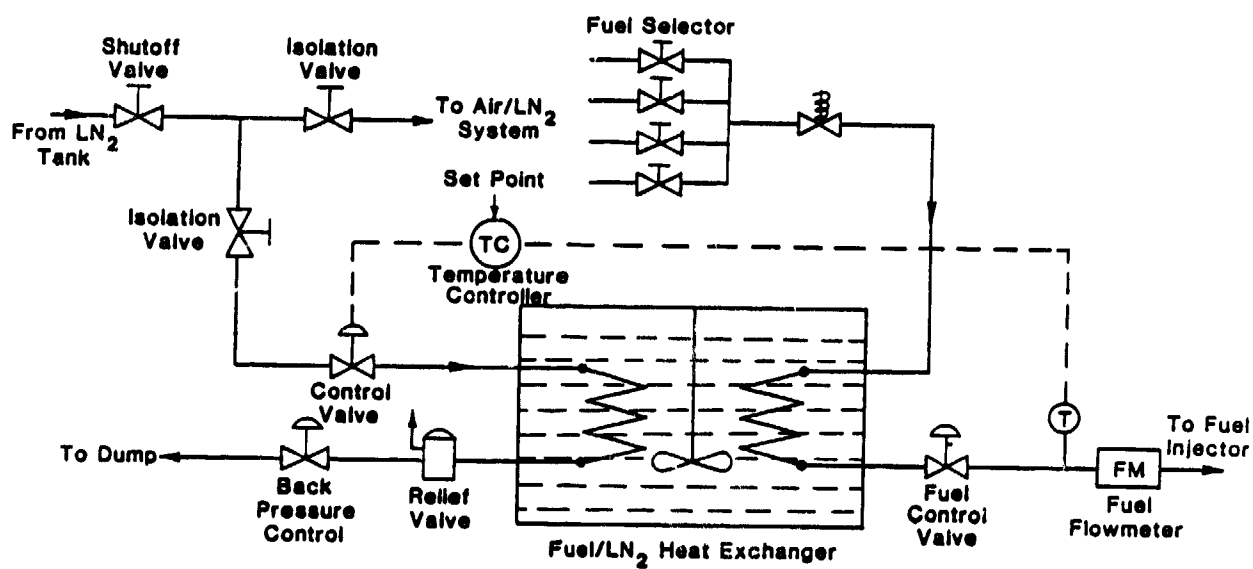


Figure 17. Altitude-Relight Facility Fuel-Cooling System.

5.0 TEST PROCEDURES

5.1 DROPLET MEASUREMENT

Droplet measurements were made using the Spectron droplet-sizing interferometer (DSI) described earlier. Prior to each run, the instrument was calibrated using a monosize-droplet generator. The nozzle was mounted in the stand such that the spray was oriented vertically downwards. The droplet measurements were conducted on a horizontal plane 50.8 mm downstream of the nozzle exit plane. The probe volume was traversed along a diameter of the spray in this plane. The capability of the DSI instrument was fully utilized by making detailed measurements at several points in each traverse, thus assuring a representative number for SMD.

At each measurement location the instrument yields the following values:

t_{tot}	Total time in seconds for measurements at a particular location
N_{tot}	Total number of samples at a location during a measurement period
$D_{\bar{v}}$	Volume mean diameter for the time series of droplet diameters
D_s	Surface mean diameter
D_{SMDL}	Local SMD

Consider a measurement point at a radial position r . Let the cross-sectional area of the probe volume (normal to the spray axis) be A_ϕ ; then:

the number of droplets passing through the probe volume per unit time = $N_s = N_{\text{tot}}/t_{\text{tot}}$,

the number of droplets per unit time passing through an annular area, $2\pi r dr$, including the probe volume = $N_s \times 2\pi r dr / A_\phi$,

and overall SMD (only one horizontal plane is considered here) is

$$= \frac{\int N_s D_{\bar{v}}^3 2\pi r dr}{\int N_s D_s^2 2\pi r dr} = \frac{\sum_i N_{si} A_{\phi i} D_{vi}^3}{\sum_i N_{si} A_{\phi i} D_{si}^2}$$

5.2 ALTITUDE RELIGHT AND LEAN BLOWOUT

The major objective of this test program was to eliminate fuel physical-property effects on atomization by testing all the fuels in such a way that the spray SMD was the same for all. In addition, it was desirable to conduct the tests under conditions typical of altitude relight for engines in flight. Both the objectives were met by using individual sets of pressure-atomizing nozzles designed to give the same SMD for each fuel while flowing the rate corresponding to minimum fuel flow of the Reference engine. Table 3 is the test matrix for the pressure-atomizing nozzles, altitude-relight tests. Two temperatures were below the freezing point of Diesel 2 and were omitted for that fuel only.

Table 3. Test Conditions for Pressure-Atomization Nozzles.

Test Point	Temp (K)		Flow Rate		JP-4	Jet A	Jet A + 2040 Solvent	No. 2 Diesel
	Air	Fuel	Air, kg/s	Fuel, g/s				
1	272	272	0.522	11.6	X	X	X	X
2	272	272	0.417	11.6	X	X	X	X
3	272	272	0.313	11.6	X	X	X	X
4	261	261	0.417	11.6	X	X	X	X
5	261	261	0.336	11.6	X	X	X	X
6	261	261	0.254	11.6	X	X	X	X
7	250	250	0.281	11.6	X	X	X	Not Tested ↓
8	250	250	0.227	11.6	X	X	X	
9	250	250	0.172	11.6	X	X	X	
10	239	239	0.141	11.6	X	X	X	↓
11	239	239	0.113	11.6	X	X	X	↓
12	239	239	0.086	11.6	X	X	X	↓

The appropriate fuel nozzles were installed in the combustor prior to each pressure-atomizing-fuel-nozzle test. The fuel lines were flushed out every time a fuel change was made. The airflow corresponding to the test condition was first set, and then the air-cooling system activated to control the combustor inlet temperature. The nozzles were bypassed while the fuel temperature was brought to the required value. The combustor pressure was set at the desired level, and the ignition system was energized. Fuel flow (at the constant design value) was initiated, and ignition-thermocouple indicators were monitored for lightoff. If ignition was not achieved, the pressure was increased in small increments and the procedure repeated until a lightoff was indicated. The pressure at which this occurred was recorded as the initial (or first-cup) lightoff. The swirl cup that achieved the initial lightoff was also identified and recorded. The pressure was then gradually increased until

all five ignition thermocouples indicated a lightoff. The ignitor was turned off while monitoring of the thermocouples continued. If the combustion was sustained, it was designated full propagation, and the pressure at which it occurred was recorded. If the combustion was not sustained, the procedure was repeated until full propagation was achieved. The combustor pressure was then gradually lowered until one of the ignition indicators registered a blowout. The pressure and the designation of the swirl cup for first-cup blowout were recorded. The combustor pressure was then lowered further until all the cups blew out, and the corresponding pressure was recorded. The entire procedure from lightoff to complete blowout was repeated three times at each condition.

For the air-blast nozzles, an identical test matrix and an identical test procedure were used for initial tests with JP-4. However, ignition was achieved only at 5 of the 12 test conditions. With the other fuels, no ignition was recorded in the entire test matrix. Comparison of fuel ignition performance was obviously not possible under these conditions; hence, several modifications were tried. These included moving the ignitor inwards into the combustor, attempting to lightoff at ambient pressure while the fuel flow was slowly increased, and combinations of the above. The only fuel that gave a consistent lightoff was JP-4. It was then decided to increase the temperature to the ambient value and attempt the tests. As with the pressure-atomizing nozzles, fuel flow was set at the design value, and pressure was increased in small increments until lightoff was observed. It was not possible to achieve repeatable full propagation for Jet A, blended Jet A and 2040 Solvent, or No. 2 Diesel. Hence, the testing was restricted to initial lightoff at ambient fuel and air temperatures at the design fuel-flow rates.

6.0 TEST RESULTS

6.1 DROPLET MEASUREMENT

The droplet-measurement results for the pressure-atomizing nozzles designed for Jet A are shown in Table 4. At the design fuel flow of 2.3 g/s per nozzle, the overall SMD at ambient conditions was 47 μm . When corrected for temperature, using the correlation of Jasuja (Reference 12), the corrected SMD at 256 K and 0.1 MPa was 56 μm and met the atomization criterion for the pressure-atomizing nozzles. Droplet measurements with the other fuels using pressure-atomizing nozzles could not be completed due to an unanticipated facility failure. However, the results for Jet A indicate that the nozzle design methodology used to obtain the specified SMD for the given fuel flow, temperature, and pressure conditions is reliable and could be expected to meet the design criteria for the other fuels as well.

Table 4. Pressure-Atomizing Nozzle SMD Measurements (Jet A).

<u>Fuel Flow, g/s</u>	<u>Swirler (Yes/No)</u>	<u>Pressure Drop, mm Water</u>	<u>SMD, μm</u>
2.3	No	---	47
2.3	Yes	305	52
2.3	Yes	203	59
2.3	Yes	102	58

The SMD results with Jet A for the air-blast nozzles at several fuel flow rates and air pressure drops are shown in Tables 5 and 6. A limited amount of testing was carried out with Diesel 2 and blended Jet A + 2040 solvent fuels; these results are shown in Table 7. It is seen that the SMD increases with decreasing pressure drop. It appears that for the air-blast fuel nozzle, fuel flow rate has little effect on the SMD within the range of fuel flow tested. Furthermore, the Table 7 data indicate that, in conjunction with the swirler, the air-blast nozzle produces essentially the same level of atomization for the three fuels tested. It also appears that the air-blast nozzle does not atomize the fuel as effectively as the pressure-atomizing nozzles.

Table 5. Air-Blast Nozzle SMD Measurements, Effect of Fuel Flow Variation (Jet A).

<u>Fuel Flow, g/s</u>	<u>Swirler (Yes/No)</u>	<u>Pressure Drop, mm Water</u>	<u>SMD, μm</u>
2.3	No	508	72
2.9	No	508	72
3.5	No	508	77

Table 6. Air-Blast Nozzles SMD Measurements, Effect of of Air Pressure Drop (Jet A).

<u>Fuel Flow, g/s</u>	<u>Swirler (Yes/No)</u>	<u>Pressure Drop, mm Water</u>	<u>SMD, μm</u>
2.3	No	287	94
2.3	No	795	79
2.3	No	1143	73

Table 7. Air-Blast Nozzle SMD Measurements, Effect of Fuel Variation.

<u>Fuel</u>	<u>Fuel Flow, g/s</u>	<u>Swirler (Y/N)</u>	<u>Pressure Drop, mm Water</u>	<u>SMD, μm</u>
Jet A	2.3	Yes	508	62
Jet A + 2040	2.3	Yes	508	66
Diesel No. 2	2.3	Yes	508	66

6.2 ALTITUDE RELIGHT AND LEAN BLOWOUT

6.2.1 Pressure-Atomizing Nozzle

During initial data analysis, it became apparent that the effects of fuel volatility on ignition and blowout total pressure were subtle in this test program, where atomization effects were eliminated, and resulting variations in lightoff and blowout pressures were quite small. Furthermore, the test conditions spanned a wide range of airflow and inlet air and fuel temperature.

A multiple-regression software package was utilized to analyze the data trends and to evaluate the statistical significance of the various independent variables such as the 10% boiling point, 50% boiling point, and flash point for the fuel volatility and inlet air temperature, inlet fuel temperature, and airflow for the combustor inlet conditions. In the early attempts, the best fit was given by a linear combination of combustor airflow and the 50% boiling point of the fuel. The correlation was then redefined in terms of air/fuel ratio and $\rho_s/\ln(1+B)$, and this correlation was found to be slightly better than the previous attempts. The coefficients and the corresponding F-ratios (which, in effect, express the degree of certainty with which the observed data variation may be associated with variation in the given variable) are listed in Table 8. The critical F-ratio was selected to be 3.0, corresponding to better than 90% confidence (that is, there is better than 90% probability that the observed variations are due to the changes in these two variables).

Table 8. Statistical Correlations for Pressure-Atomizing Nozzles.

$$PT_3 \text{ (kPa)} = a + b(f/a)^{-1} + c[\rho_s/\ln(1+B)]$$

Condition	a	b	c	F-Crit	$F[(f/a)^{-1}]$	$F[\rho_s/\ln(1+B)]$	R^2
Initial Lightoff	5.42	0.924	29.54	3.0	93.68	5.97	0.74
Full Propagation	29.96	1.106	0	3.0	233.9	---	0.85
First-Cup Blowout	26.58	0.934	0	3.0	189.8	---	0.83
Complete Blowout	16.91	0.884	14.67	3.0	187.1	3.51	0.84

6.2.1.1 Initial Lightoff

The combustor inlet total pressure at initial lightoff (that is, first-cup lightoff) for JP-4 is plotted as a function of the air/fuel ratio in Figure 18. Similar data for Jet A, Jet A + 2040 solvent blend, and Diesel 2 are shown in Figures 19 through 21. As shown in the Test Matrix (Table 3), all the testing was conducted at the same design fuel flow (11.6 g/s); hence, the abscissa in this and the following similar curves is equivalent to dome airflow or primary-zone velocity (with minor corrections for the density) within a multiplicative constant.

It is clearly evident that, under the conditions tested, fuel or air temperature have no effect on lightoff total pressure (except, perhaps, for Diesel 2 at 272 K). The lightoff total pressure is generally seen to increase linearly with air/fuel ratio, indicating a direct relationship with dome velocity or an inverse relationship with fuel/air ratio. Since the objective of the program was to compare the effects of the different fuels while holding the atomization level the same at combustor minimum fuel flow and maintaining the combustor airflow at the predetermined schedule, it was not possible to separate the fuel/air ratio and dome velocity effects without an additional parameter test matrix.

In Figure 22, composite data are shown for all four fuels for initial lightoff. It is evident that the fuel volatility effect is subtle and is barely observable. The composite initial lightoff results for all four fuels have been plotted in Figure 23 using the correlation parameter

$$a + b(f/a)^{-1} + c[\rho_s/\ln(1+B)]$$

as the abscissa.

6.2.1.2 Full Propagation

The results for full propagation for the various fuels are shown in Figures 24 through 27. As in the preceding figures, the abscissa is (fuel/air

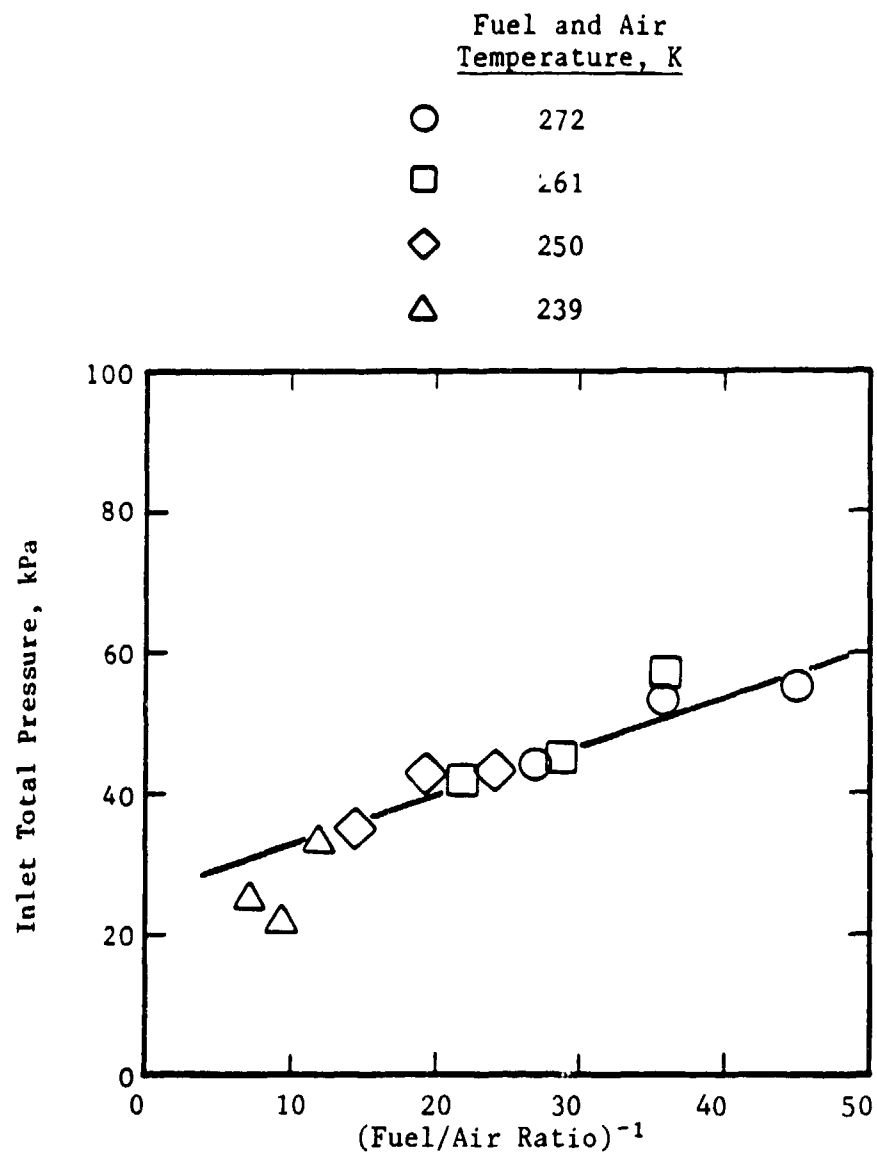


Figure 18. Pressure-Atomizing Nozzle Results; Lightoff Characteristics for JP-4 Fuel.

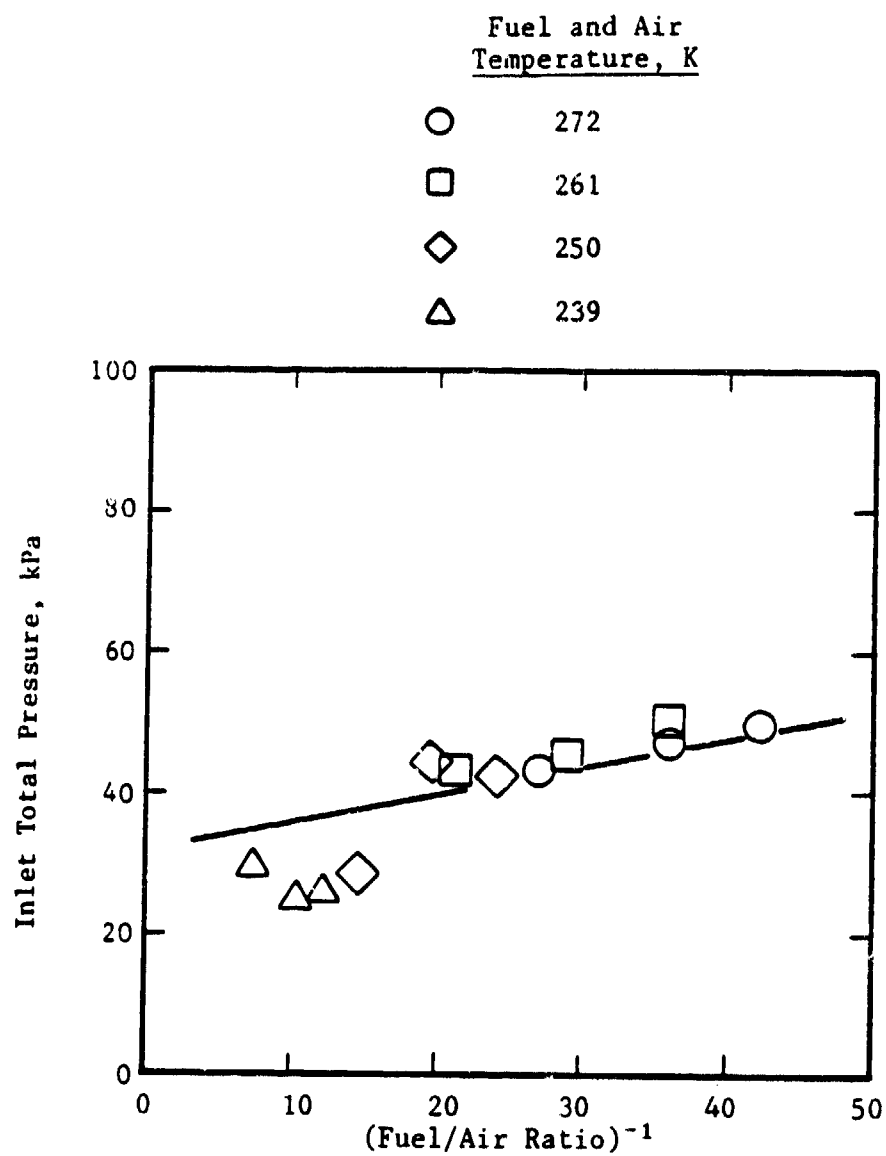


Figure 19. Pressure-Atomizing Nozzle Results; Lightoff Characteristics for Jet A Fuel.

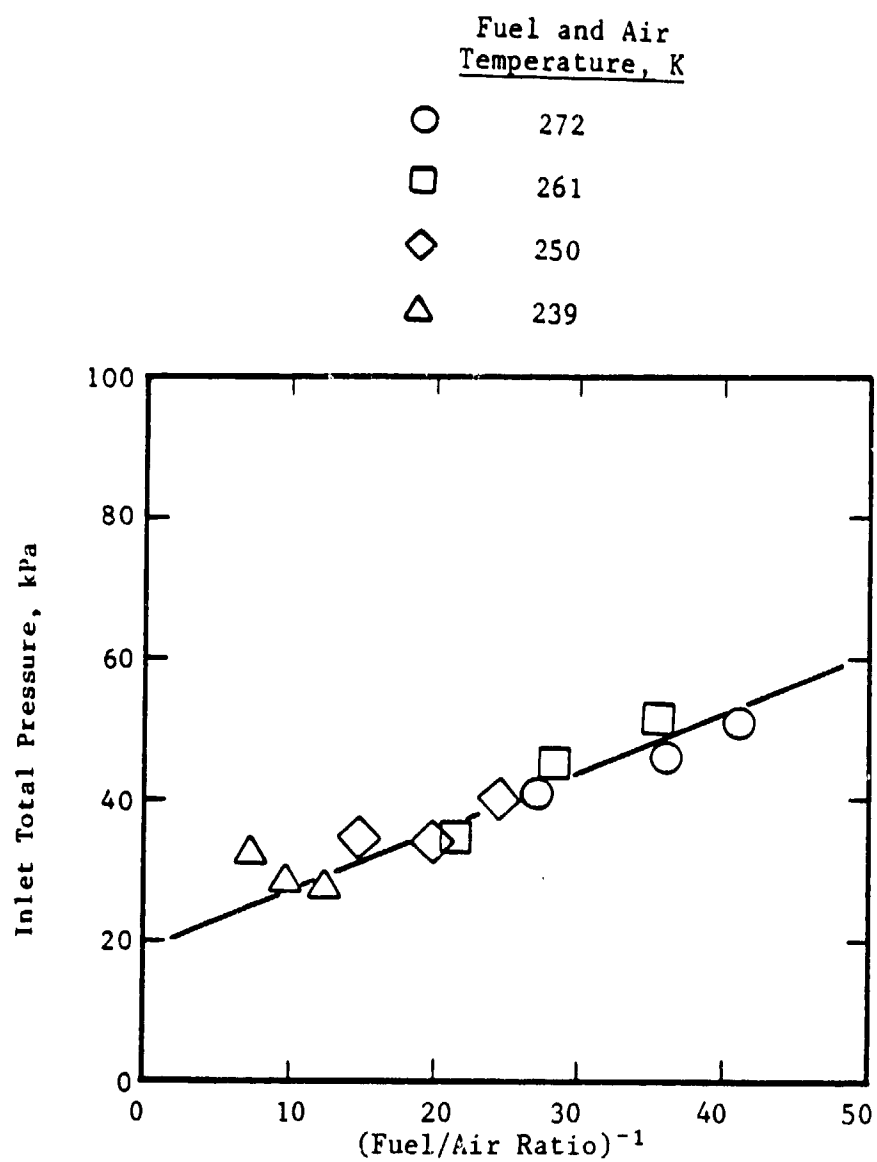


Figure 20. Pressure-Atomizing Nozzle Results; Lightoff Characteristics for Jet A + 2040 Solvent.

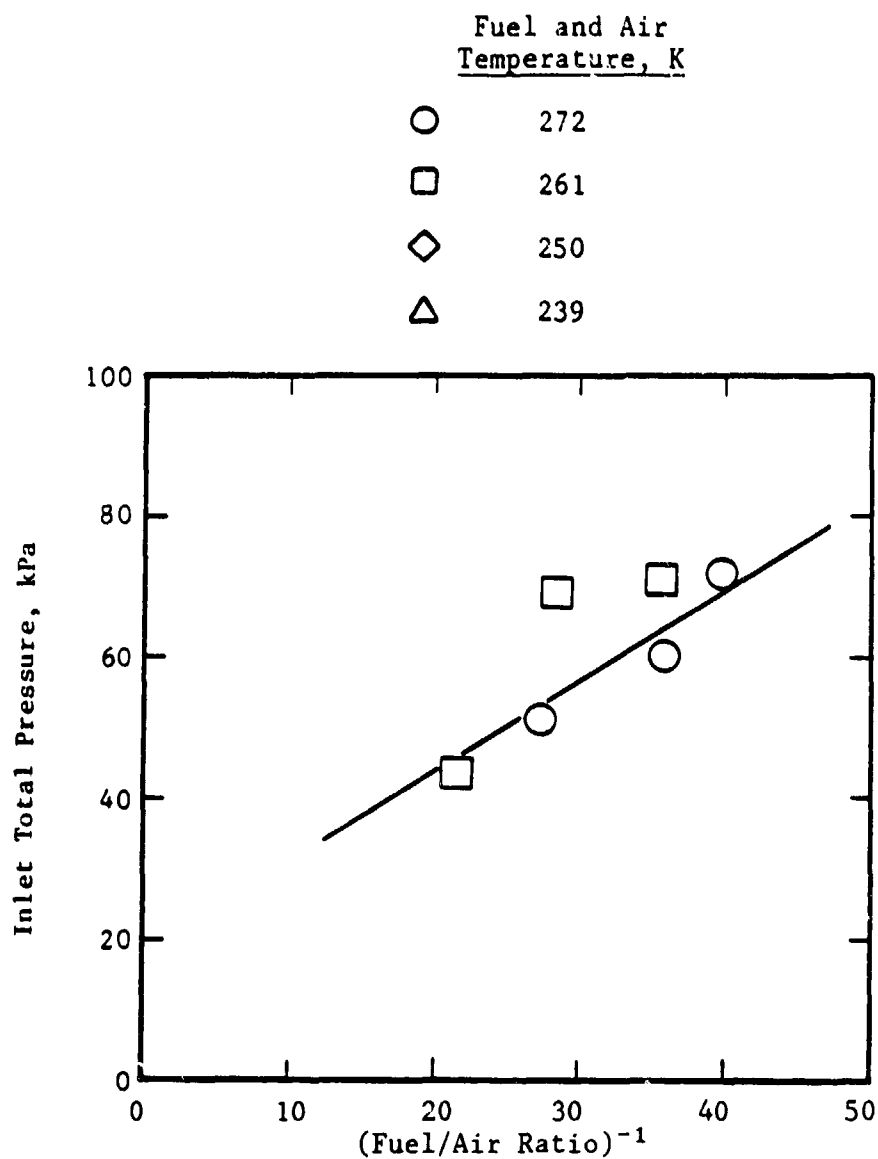


Figure 21. Pressure-Atomizing Nozzle Results; Lightoff Characteristics for No. 2 Diesel Fuel.

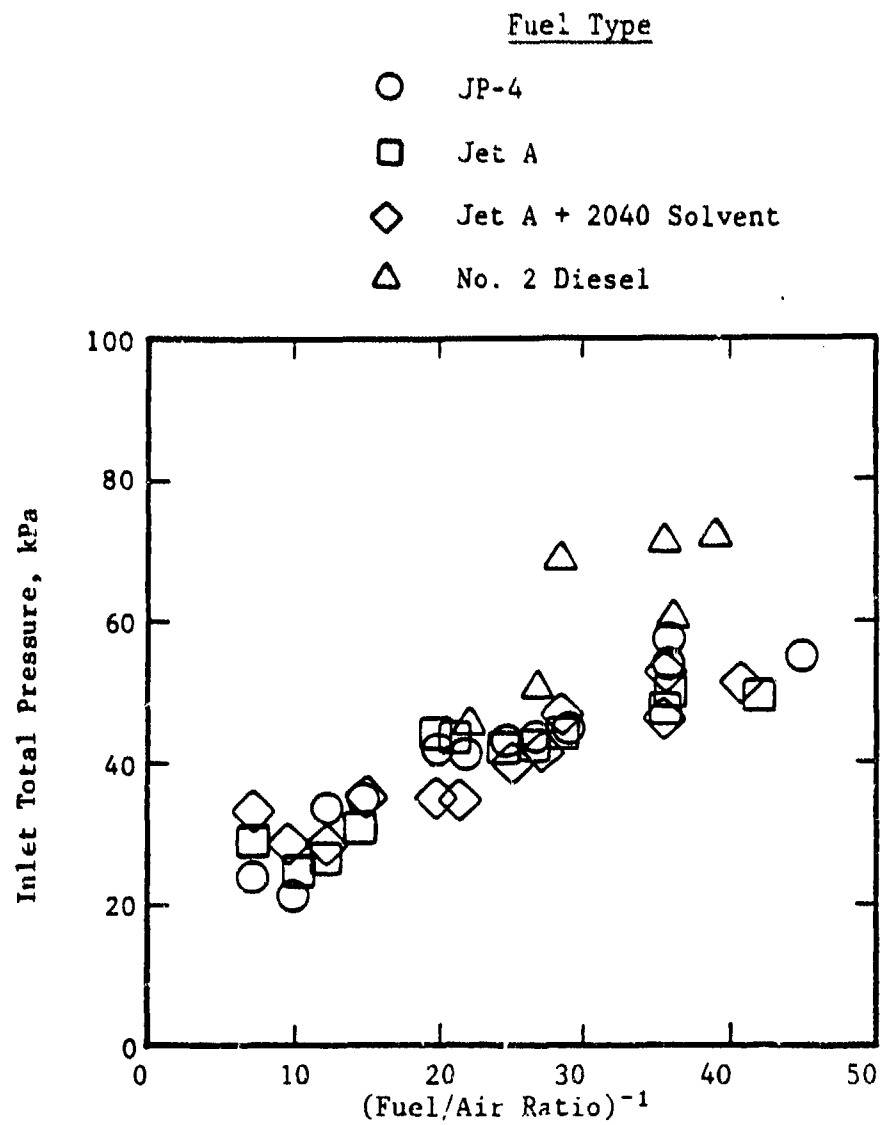


Figure 22. Pressure-Atomizing Nozzle Results; Lightoff Characteristics for All Fuels Tested.

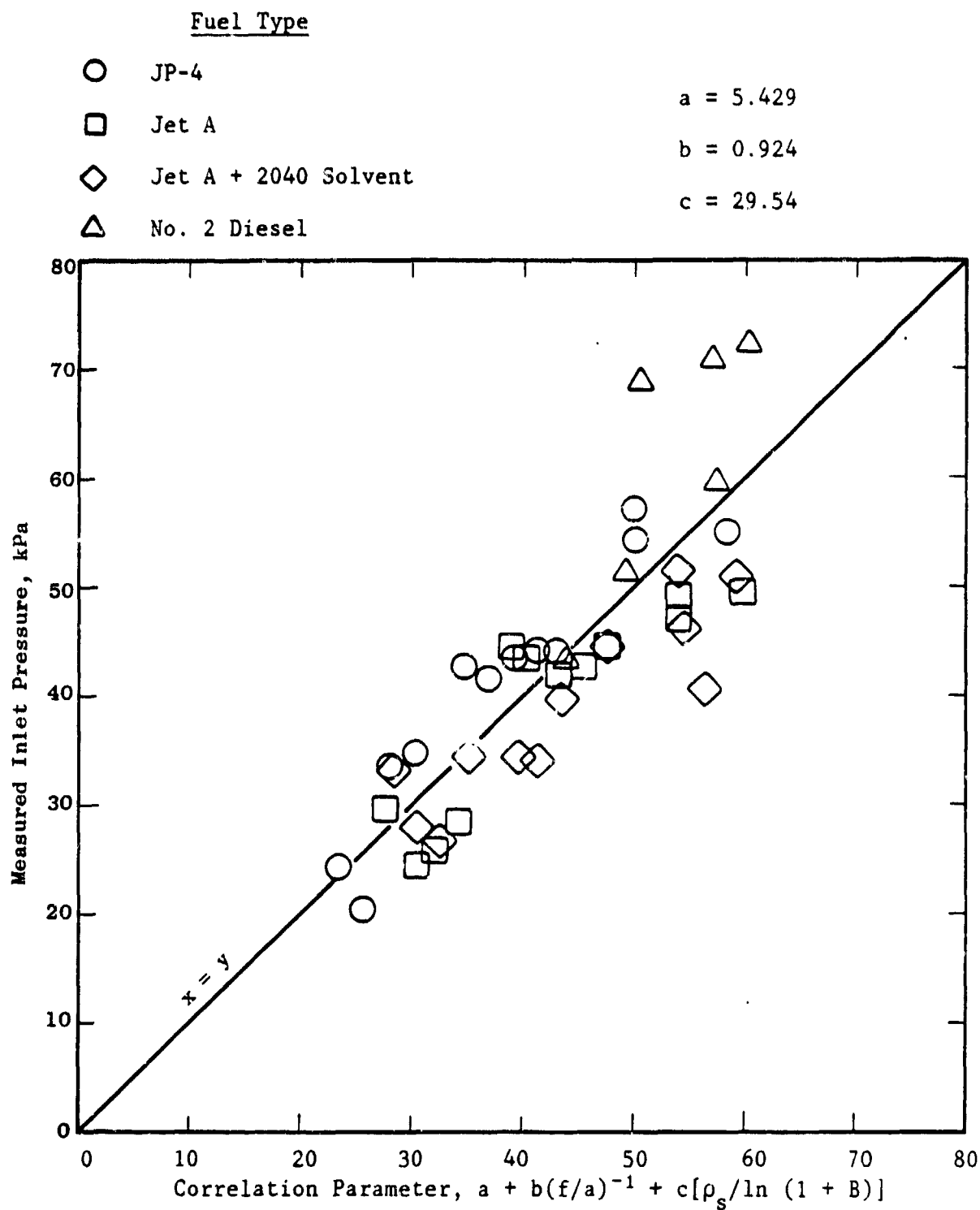


Figure 23. Pressure-Atomizing Nozzle Results; Lightoff Correlation for All Fuels Tested.

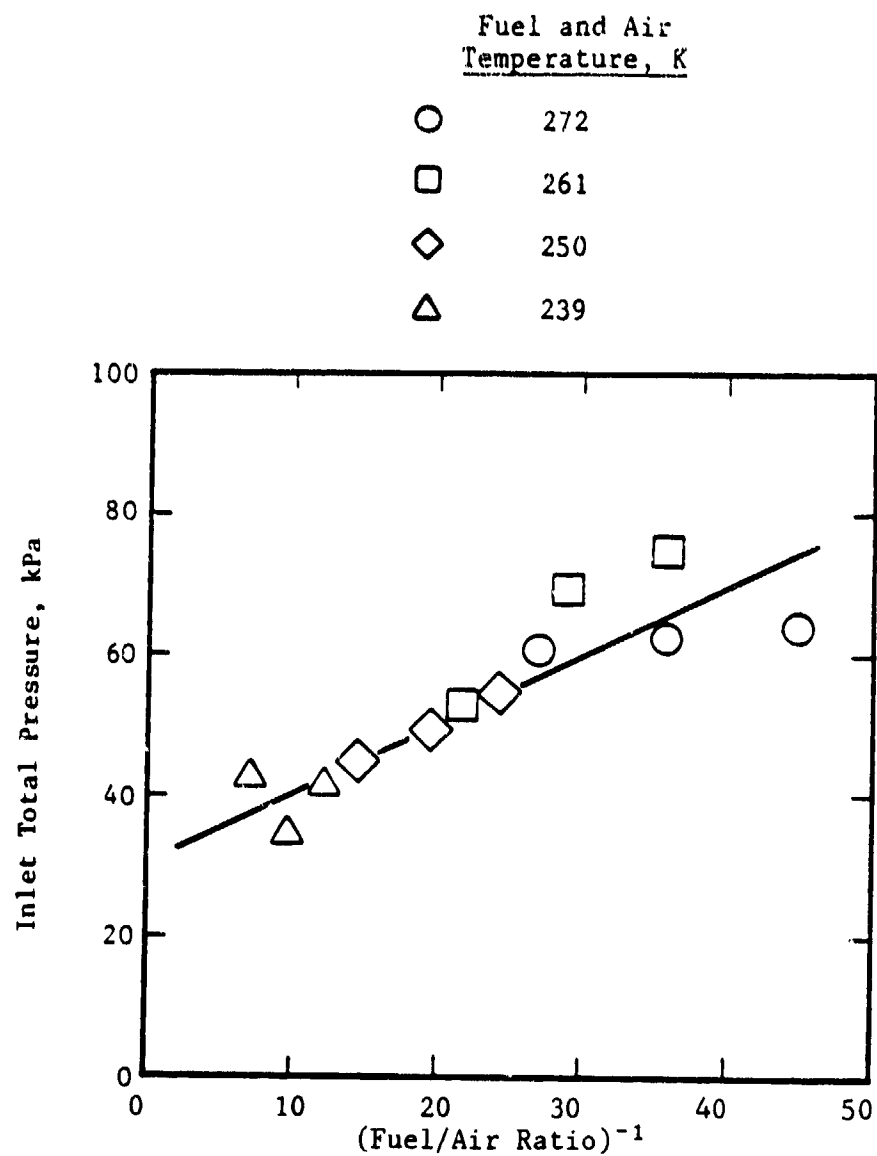


Figure 24. Pressure-Atomizing Nozzle Results; Full-Propagation Characteristics for JP-4 Fuel.

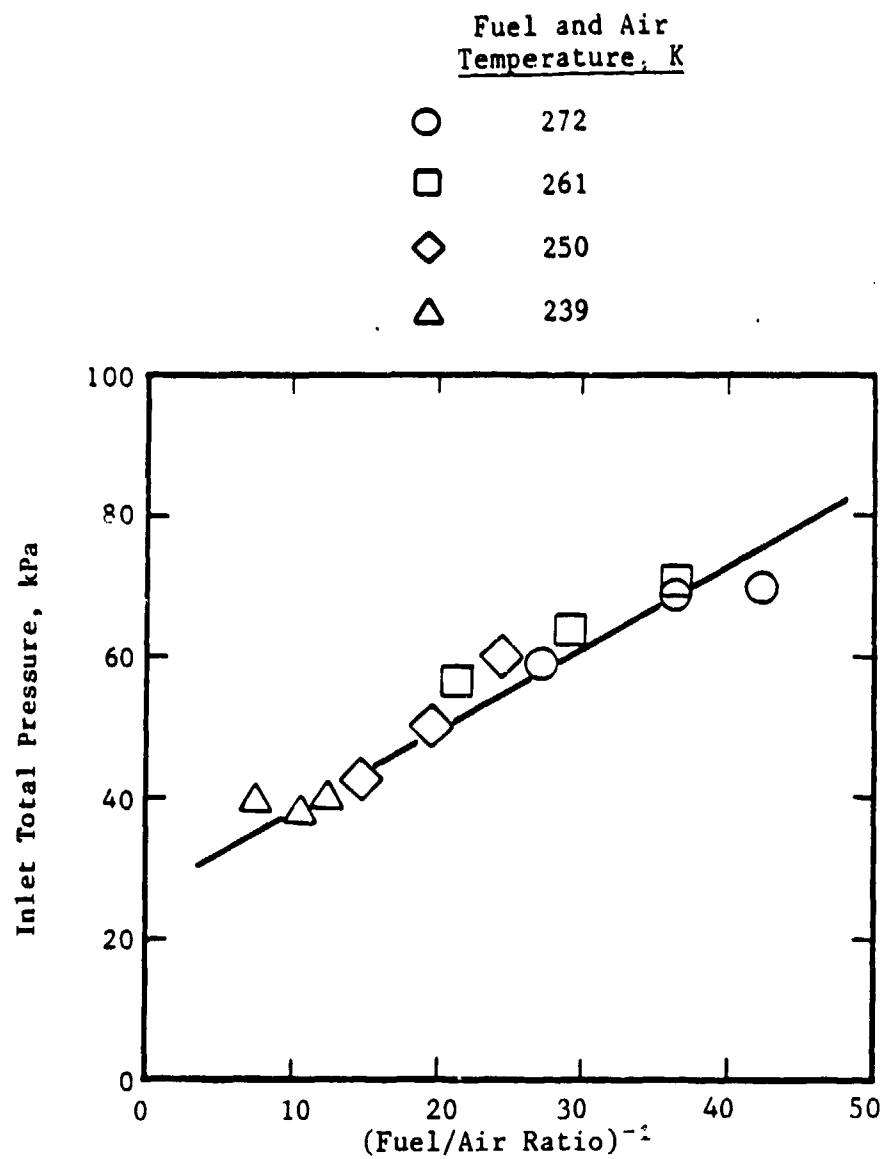


Figure 25. Pressure-Atomizing Nozzle Results; Full-Propagation Characteristics for Jet A Fuel.

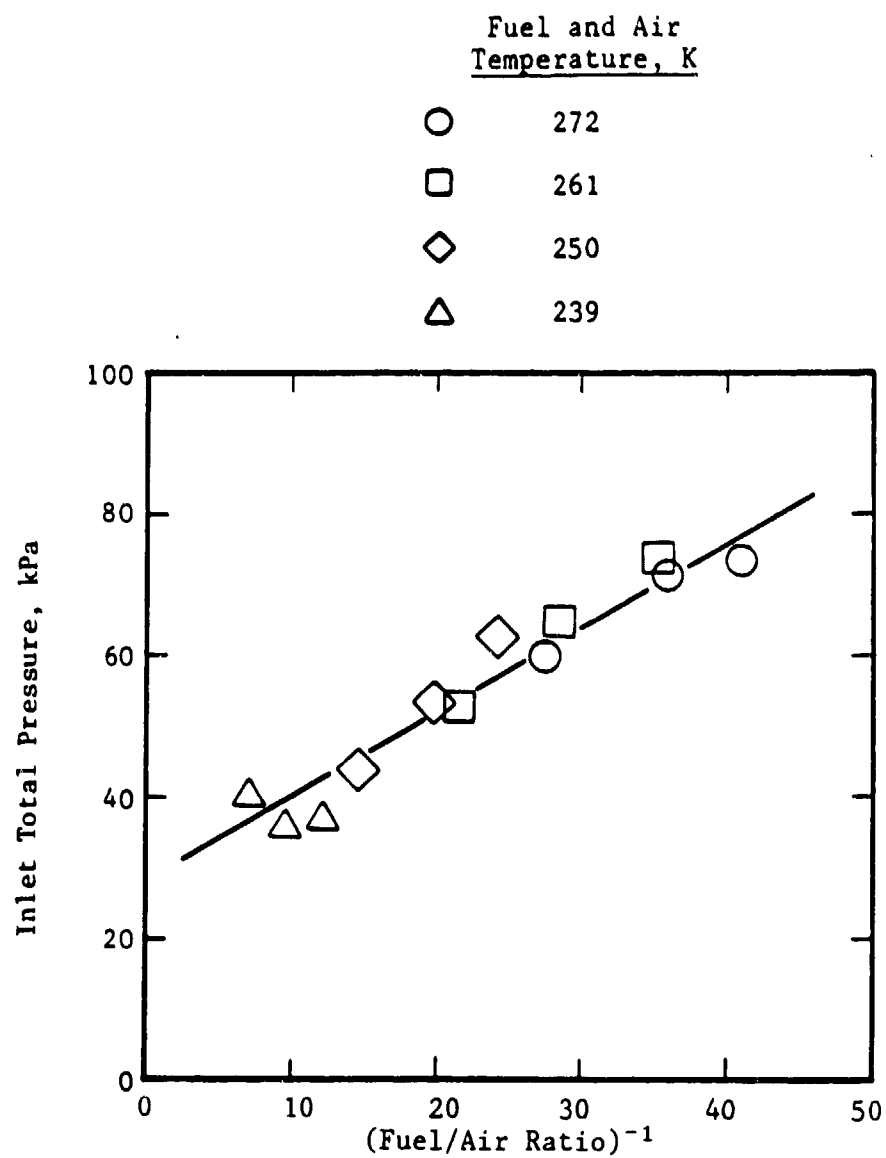


Figure 26. Pressure-Atomizing Nozzle Results; Full-Propagation Characteristics for Jet A + 2040 Solvent.

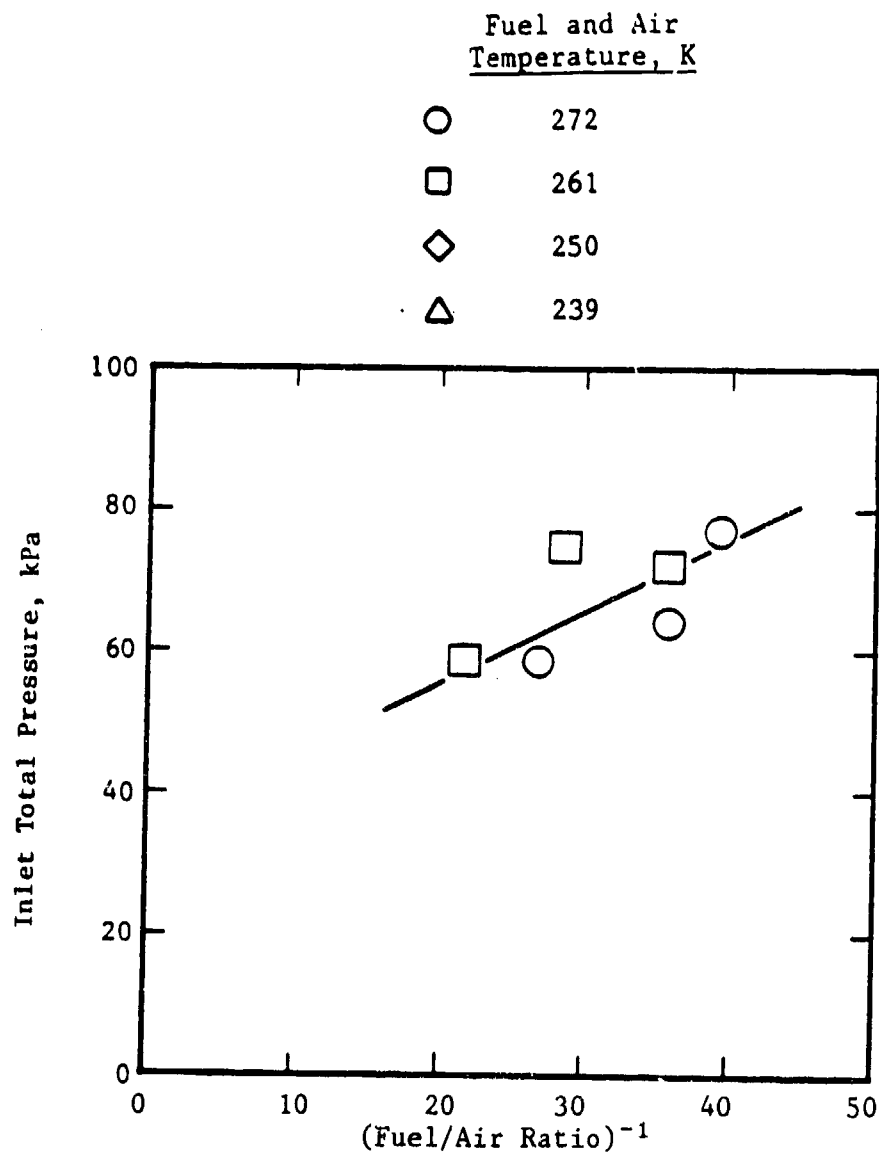


Figure 27. Pressure-Atomizing Nozzle Results; Full-Propagation Characteristics for No. 2 Diesel Fuel.

ratio)⁻¹. Again, temperature dependence is virtually absent. Figure 28 shows the results for all the fuels. Compared to the initial lightoff results, the full-propagation results are tightly clustered in a narrow band. In fact, multiple regression results indicated the fuel volatility parameters did not make a significant contribution to the correlation. Figure 29, showing the overall correlation, indicates that only combustor fuel/air ratio (or, equivalently, the combustor mass flow) is the dominant variable and that fuel volatility properties are not important for the phenomenon of full propagation from a lit swirler.

6.2.1.3 First-Cup Blowout

The results for first-cup blowout for each fuel are shown in Figures 30 through 33. The results for all four fuels are combined in Figure 34. The trend is similar to that of full propagation (Figure 28); the fuel volatility is not a key variable for first-cup blowout in this case. This conclusion is also evident from Figure 35 where the data are plotted against the statistical correlation which does not include fuel volatility characteristics.

6.2.1.4 Complete Blowout

The results for complete blowout (that is, when the flame is completely extinguished) are presented in Figures 36 through 40. The fuel volatility has some influence on complete blowout, but based on the F-ratios in Table 8 it appears to be weaker than on initial lightoff. The overall correlation for complete blowout is illustrated in Figure 41.

6.2.2 Air-Blast Nozzle

As discussed earlier, the air-blast nozzles displayed poor ignition performance. The droplet measurements reported in Table 7 indicate that the SMD produced by the air-blast nozzles was about 15% greater than that of the pressure-atomizing nozzles/swirler combination at comparable flow conditions. However, it is also seen that the SMD deteriorates rapidly with decreasing pressure drop across the dome. In fact, poor ignition performance of air-blast nozzles has been reported in the literature. Lefebvre (Reference 9) attributes it to more uniform mixing of fuel and air resulting in a narrow stability range. Pressure-atomizing nozzles, on the other hand, due to poor mixing, present a wide range of equivalence ratios in the primary zone which increases the probability of having a local region in the ignition zone within the flammability limits. Lefebvre recommends a hybrid fuel-injection system that employs pressure atomization for ignition and air-blast atomization for normal operation.

Following an exploration of simple modifications of hardware and test procedure, it was determined that the improvement in performance necessary for a study of subtle fuel effects would necessitate substantial development effort. Such an elaborate project was beyond the scope of this program. The

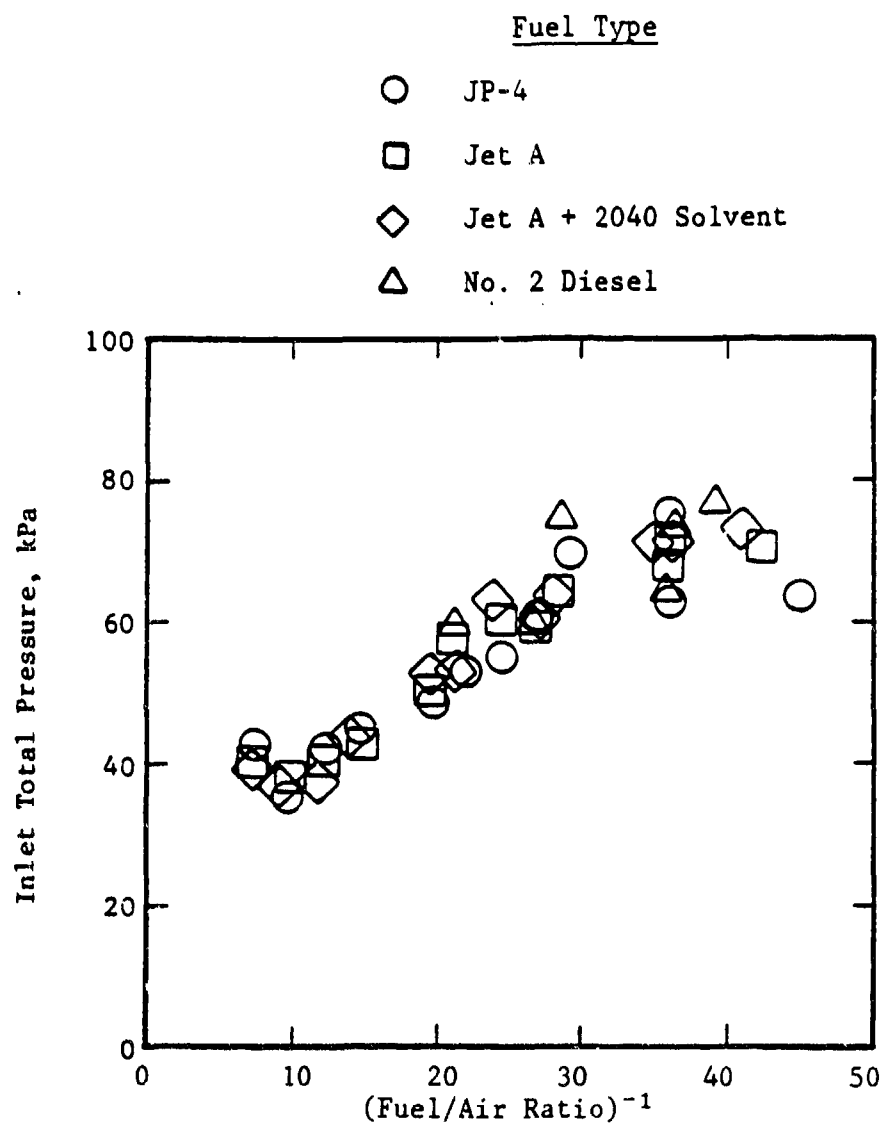


Figure 28. Pressure-Atomizing Nozzle Results; Full-Propagation Characteristics for All Fuels Tested.

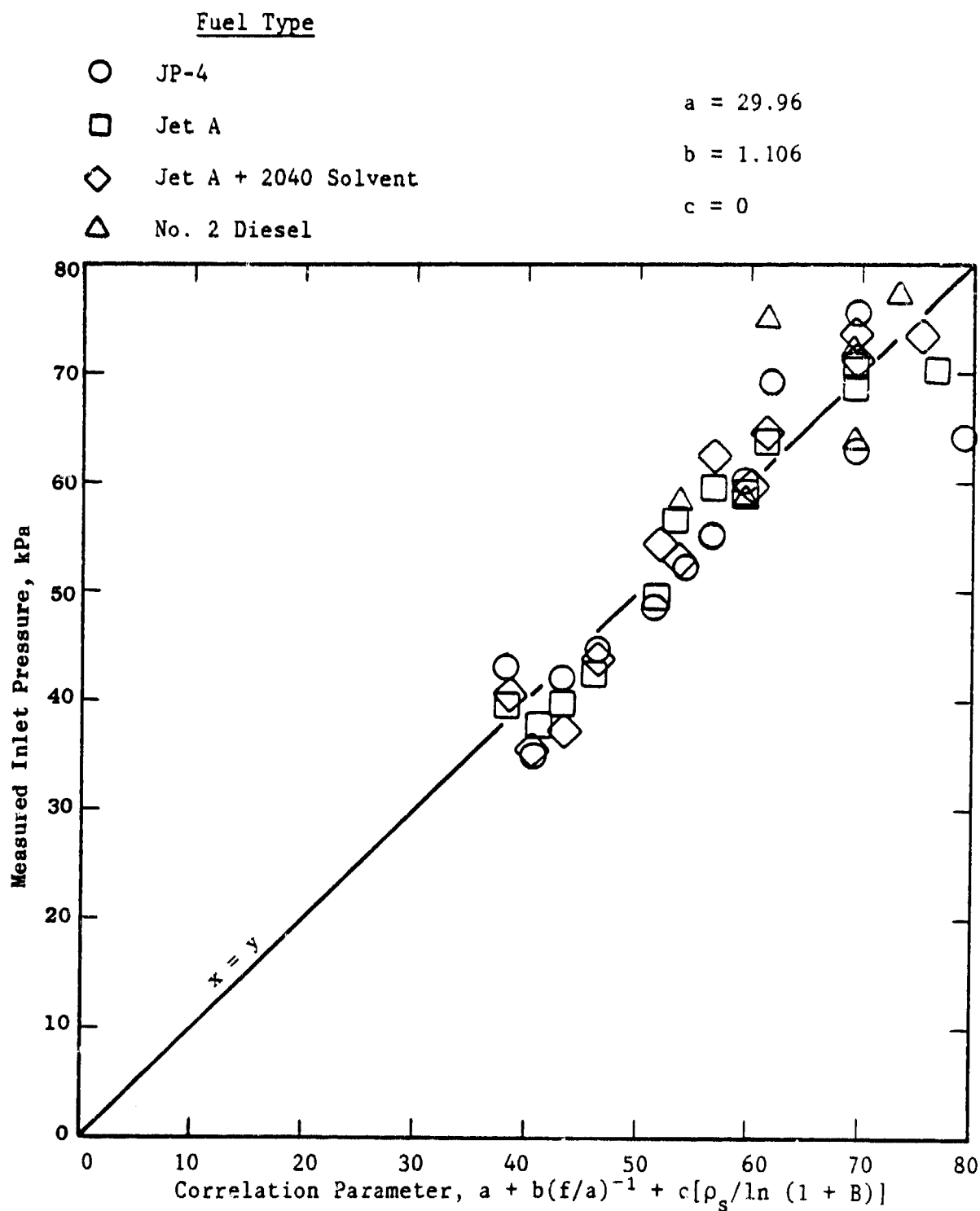


Figure 29. Pressure-Atomizing Nozzle Results; Full-Propagation Correlation for All Fuels Tested.

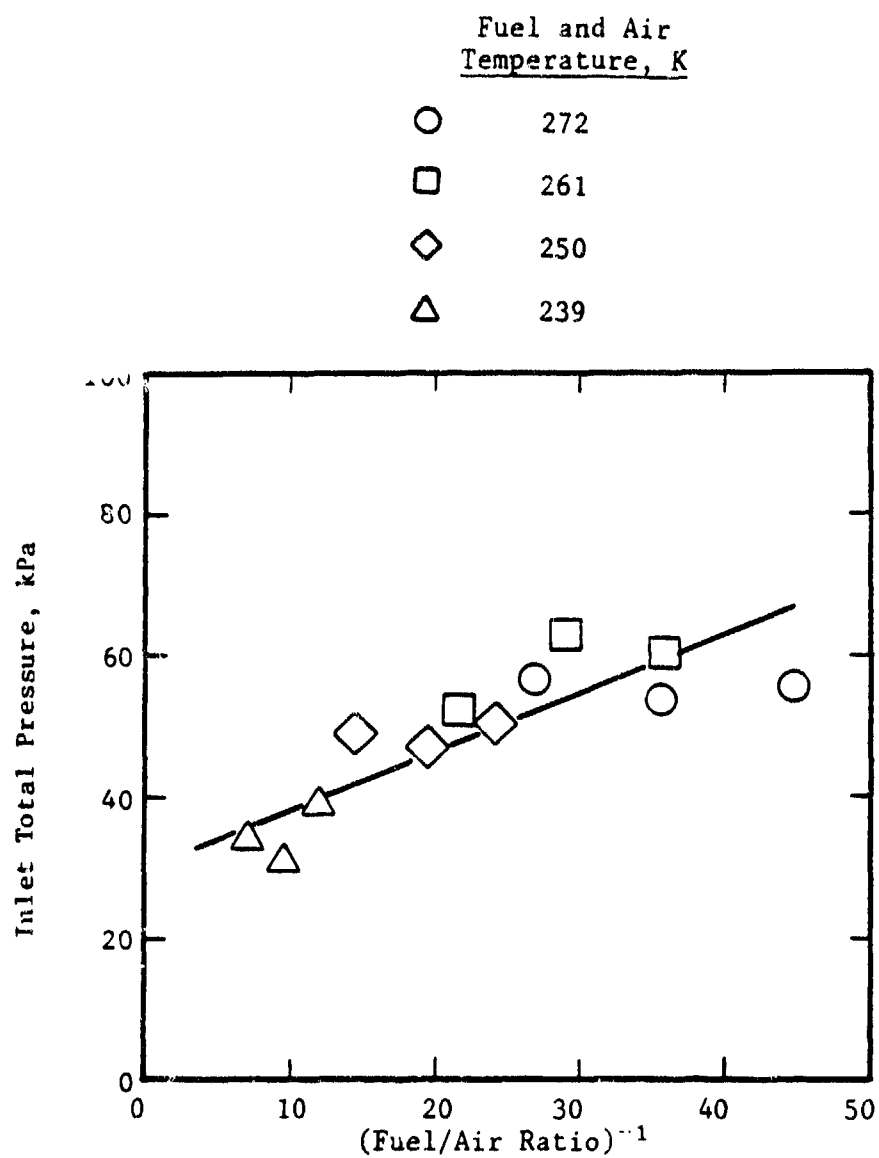


Figure 30. Pressure-Atomizing Nozzle Results; First-Cup-Blowout Characteristics for JP-4 Fuel.

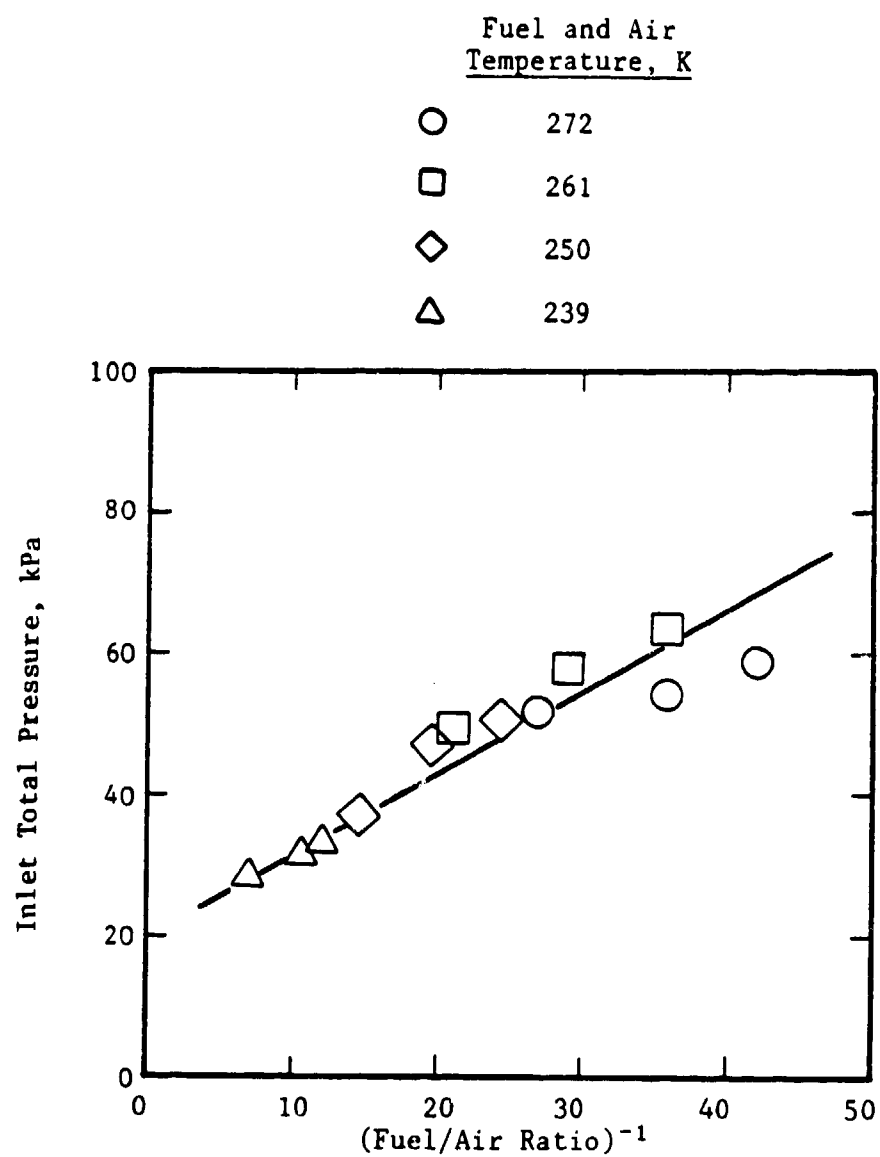


Figure 31. Pressure-Atomizing Nozzle Results; First-Cup-Blowout Characteristics for Jet A Fuel.

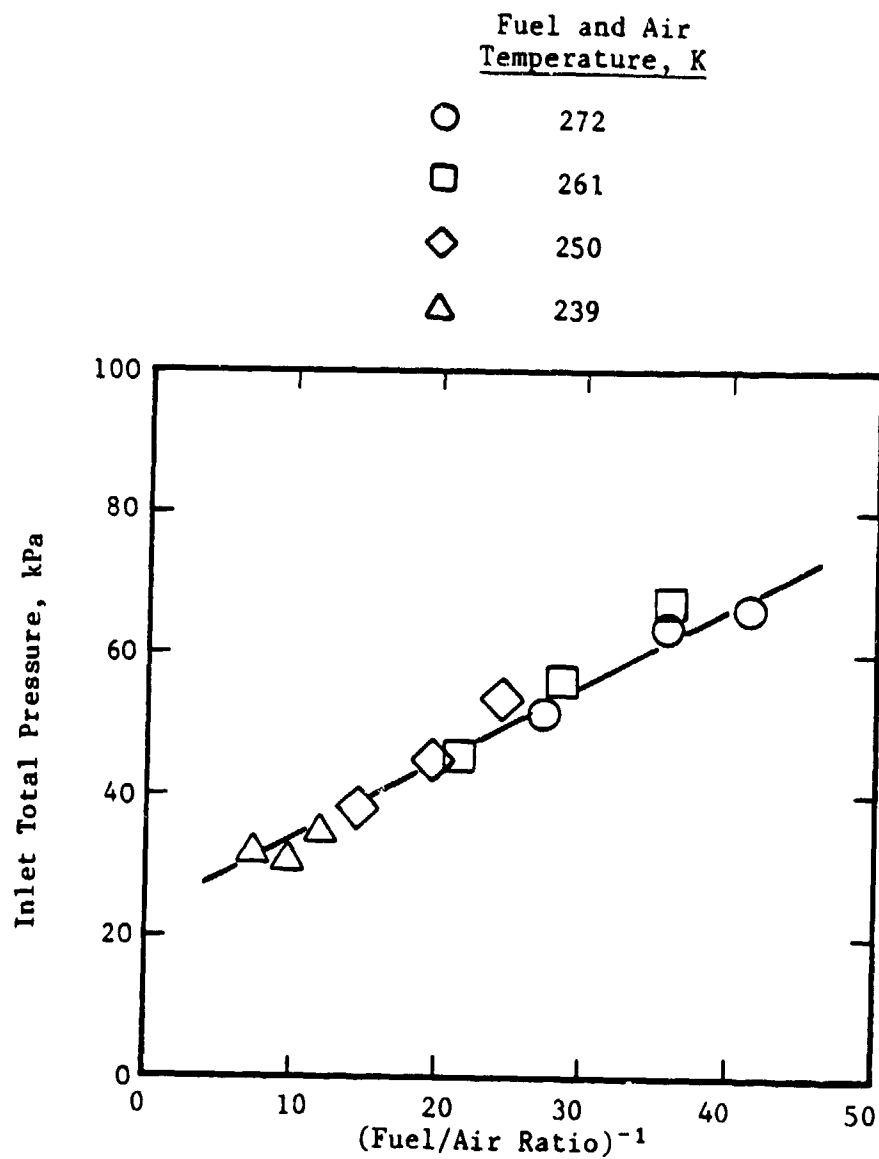


Figure 32. Pressure-Atomizing Nozzle Results; First-Cup-Blowout Characteristics for Jet A + 2040 Solvent.

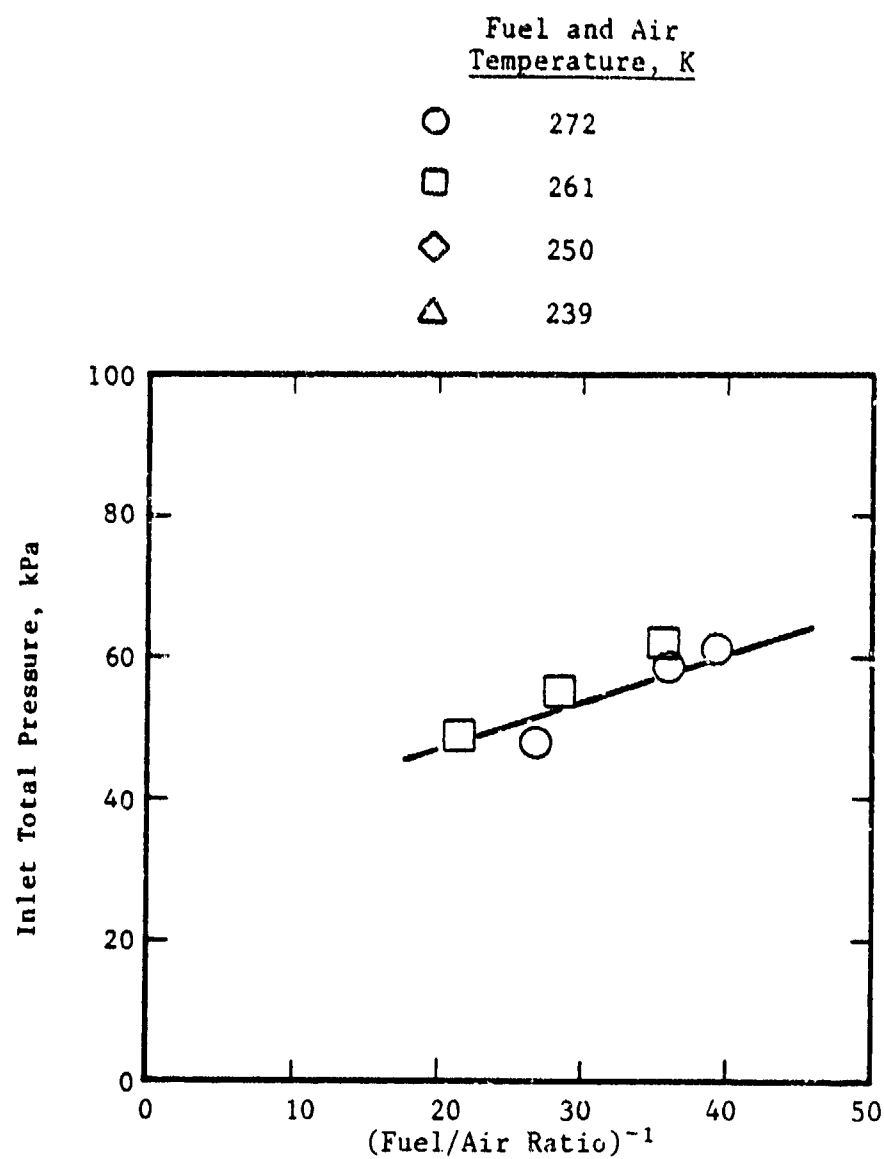


Figure 33. Pressure-Atomizing Nozzle Results; First-Cup-Blowout Characteristics for No. 2 Diesel Fuel.

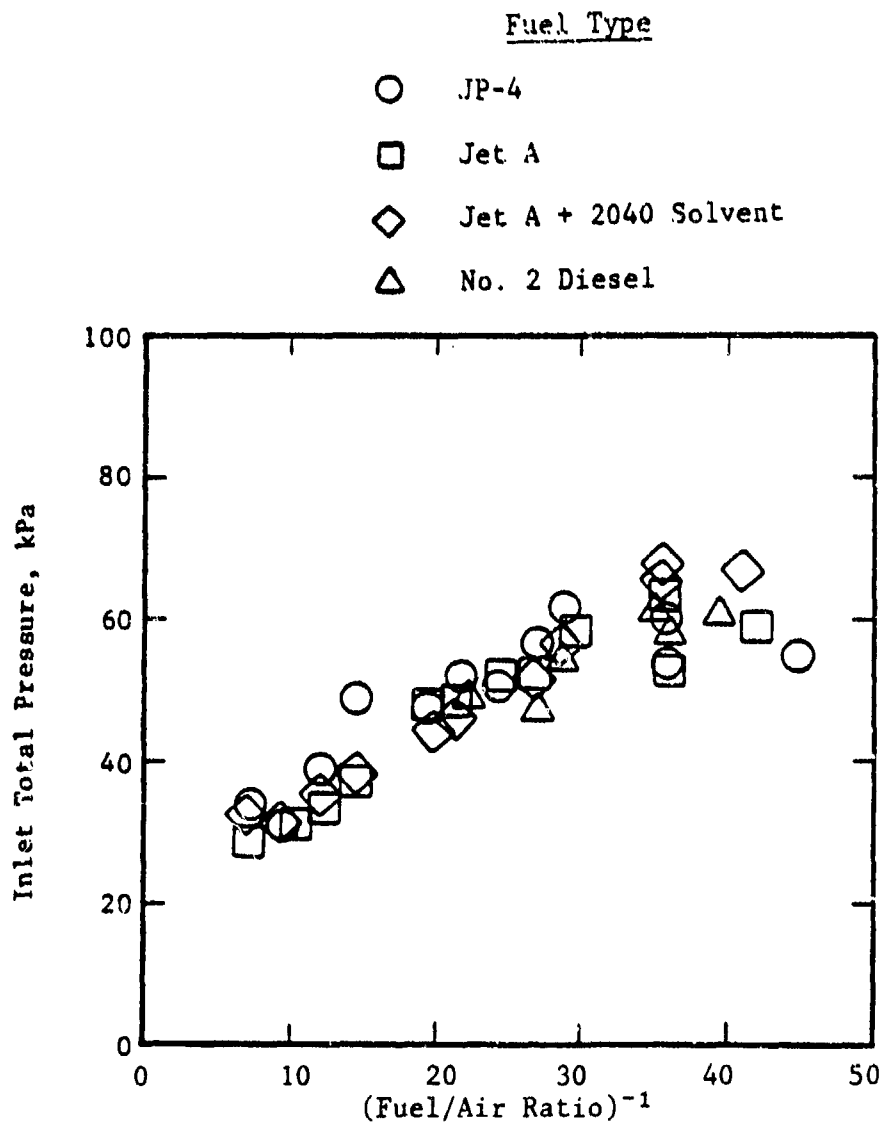


Figure 34. Pressure-Atomizing Nozzle Results; First-Cup-Blowout Characteristics for All Fuels Tested.

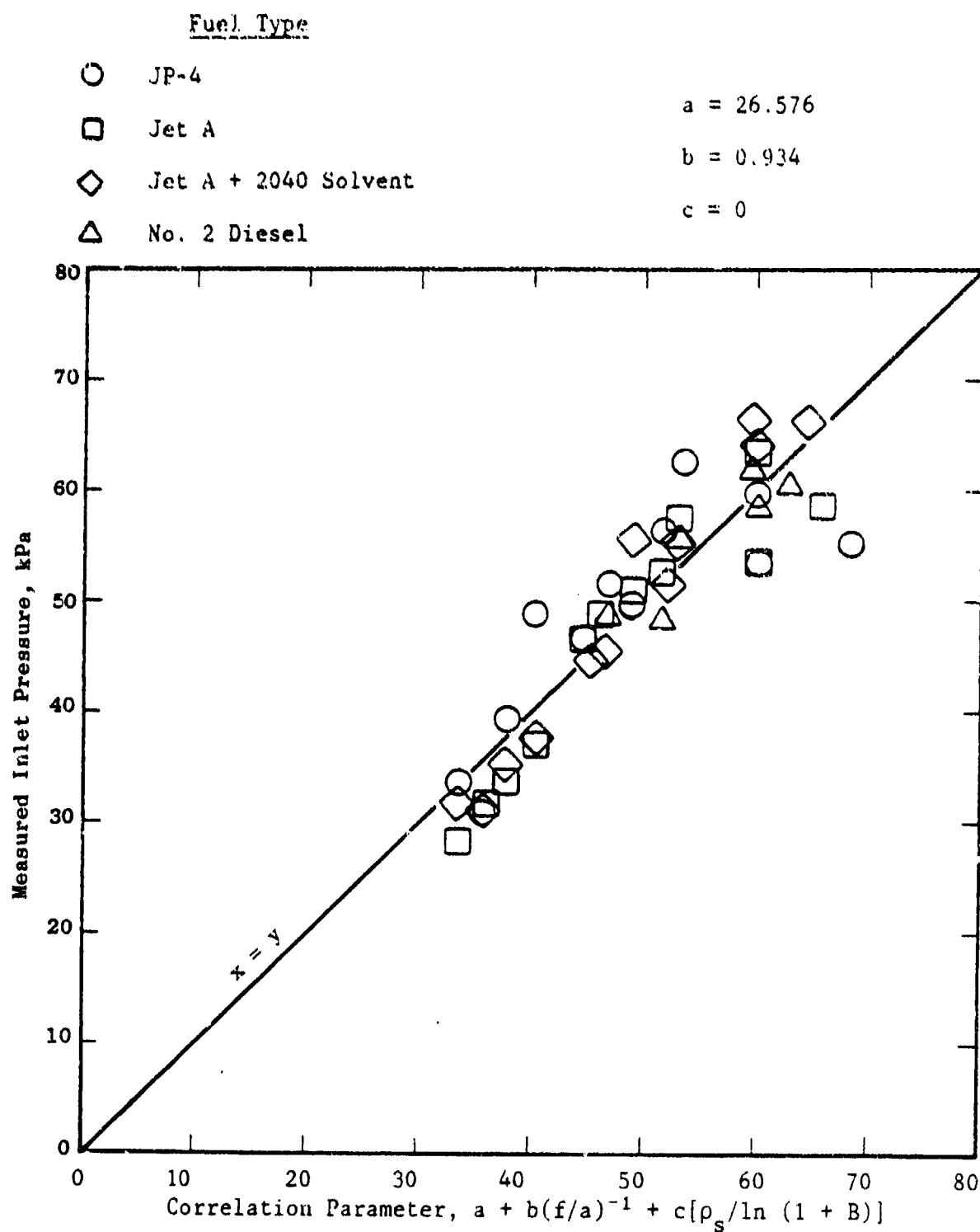


Figure 35. Pressure-Atomizing Nozzle Results; First-Cup-Blowout Correlation for All Fuels Tested.

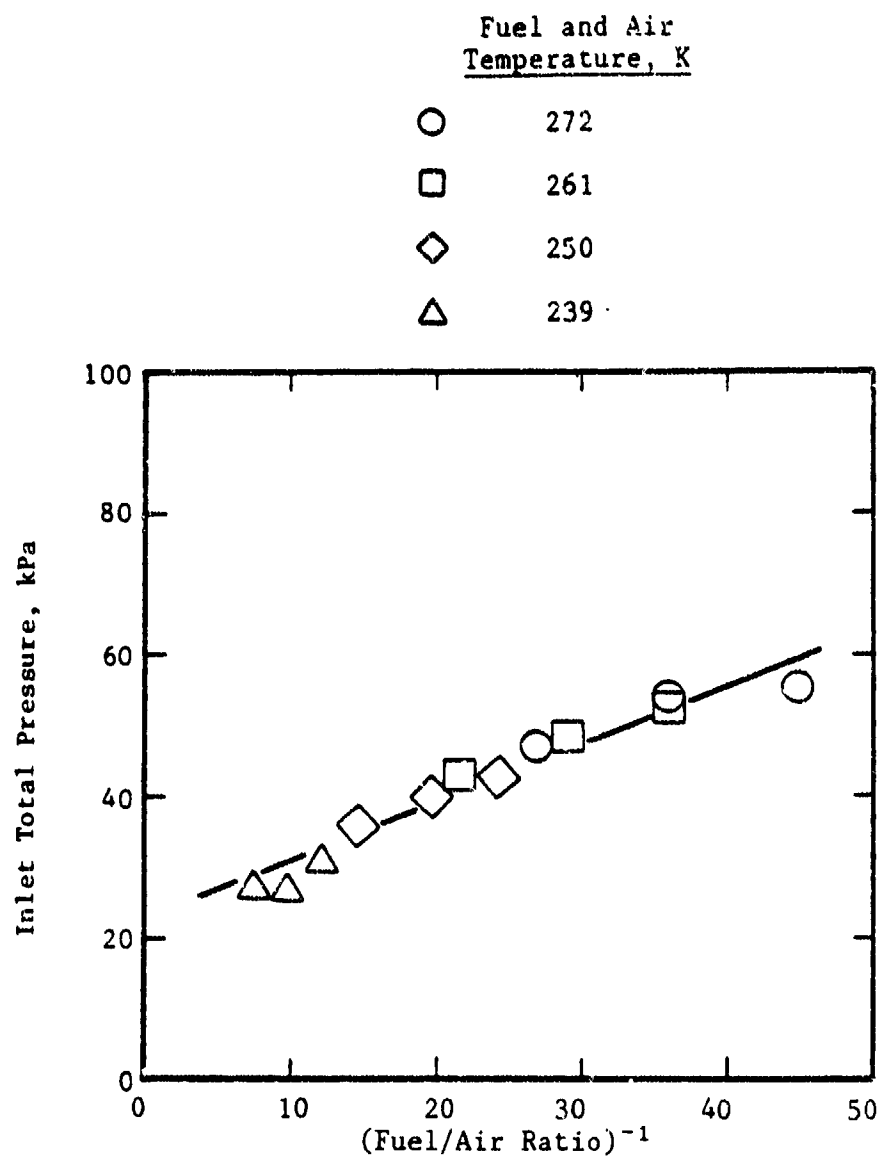


Figure 36. Pressure-Atomizing Nozzle Results; Complete-Blowout Characteristics for JP-4 Fuel.

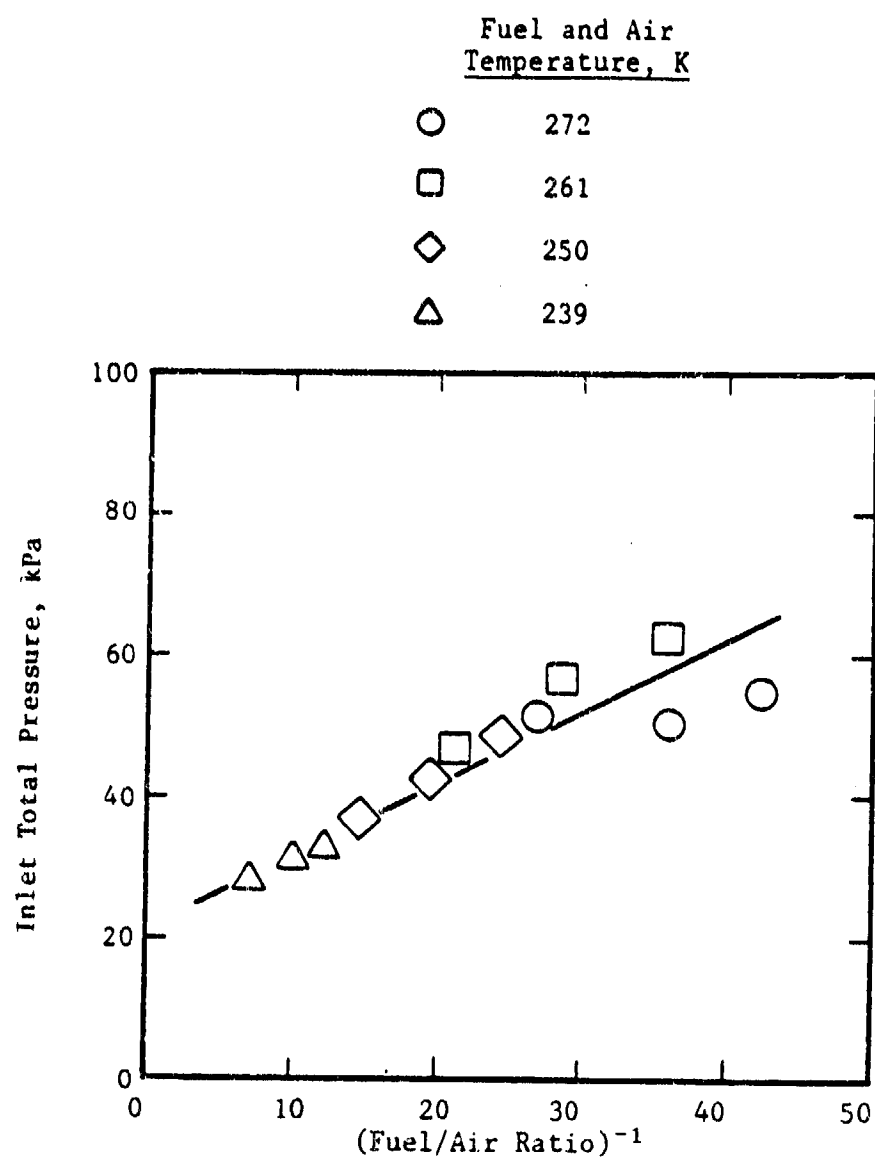


Figure 37. Pressure-Atomizing Nozzle Results; Complete-Blowout Characteristics for Jet A Fuel.

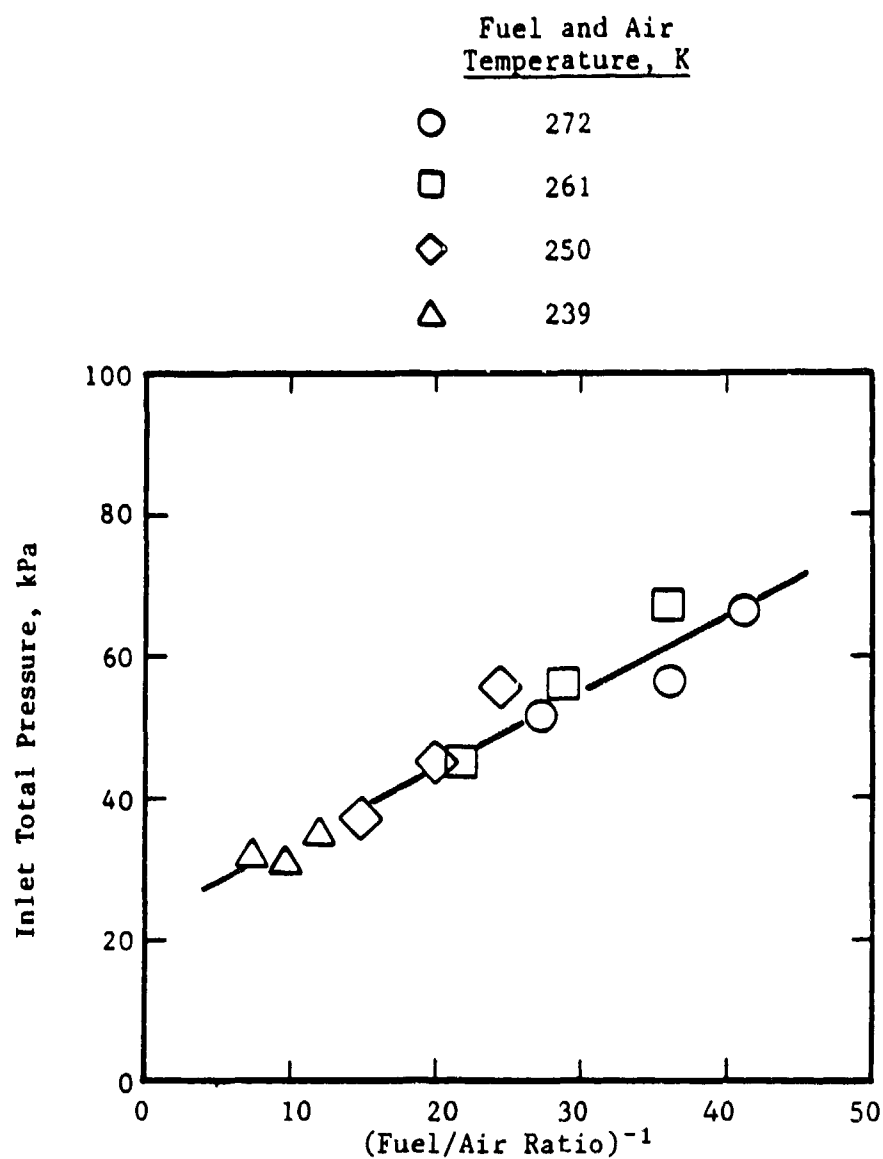


Figure 38. Pressure-Atomizing Nozzle Results; Complete-Blowout Characteristics for Jet A + 2040 Solvent.

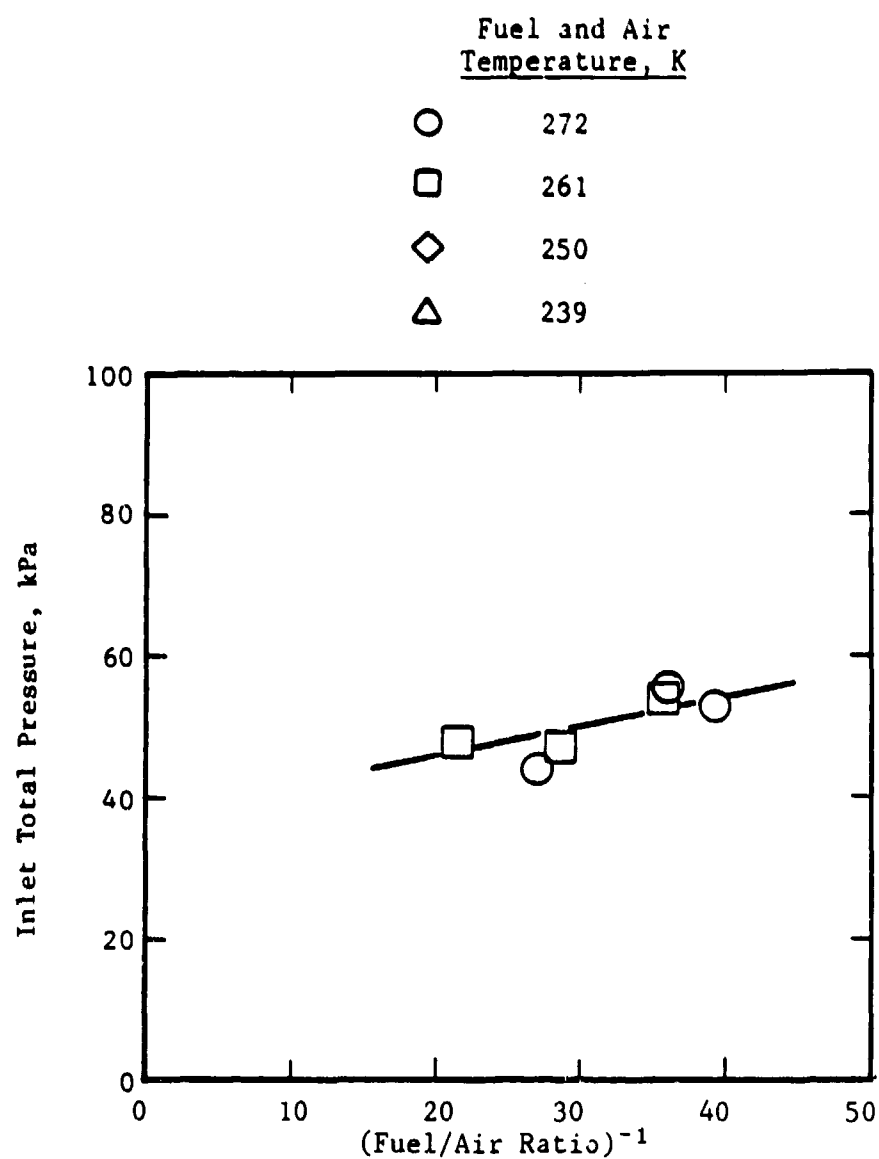


Figure 39. Pressure-Atomizing Nozzle Results; Complete-Blowout Characteristics for No. 2 Diesel Fuel.

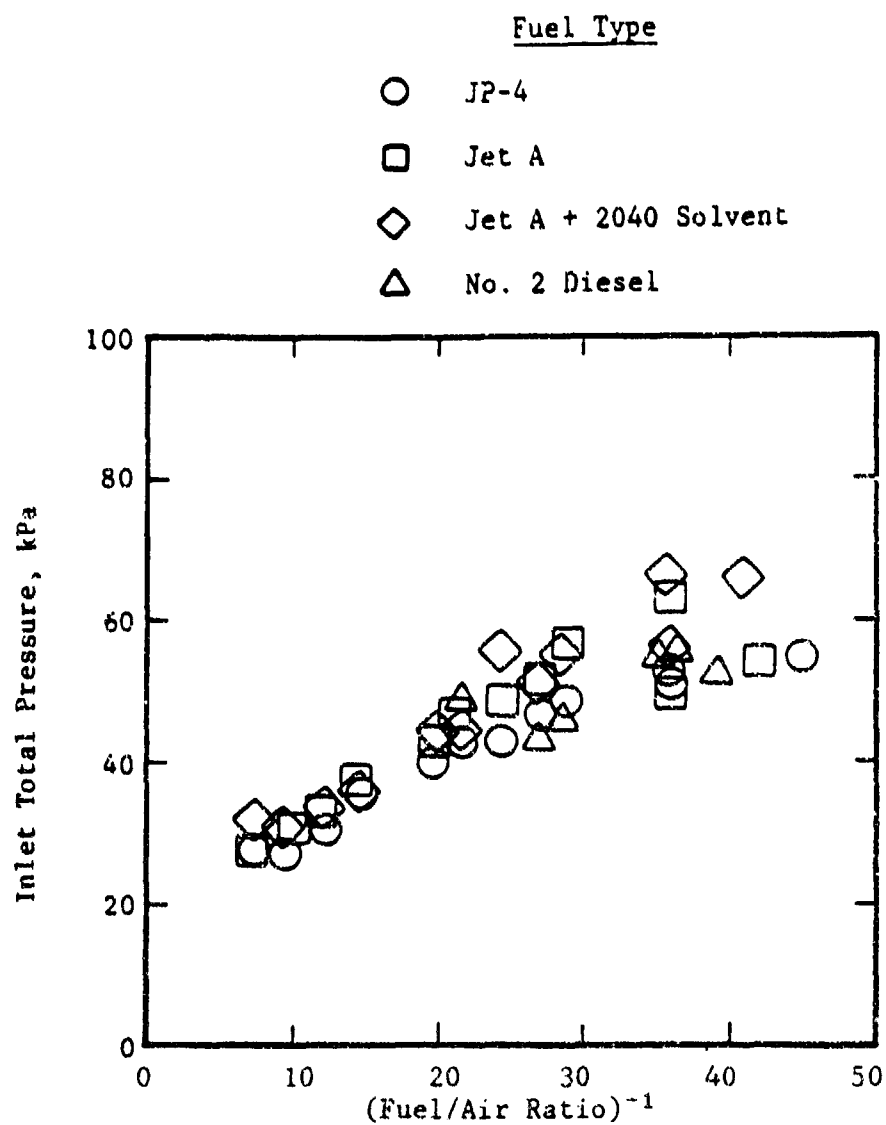


Figure 40. Pressure-Atomizing Nozzle Results; Complete-Blowout Characteristics for All Fuels Tested.

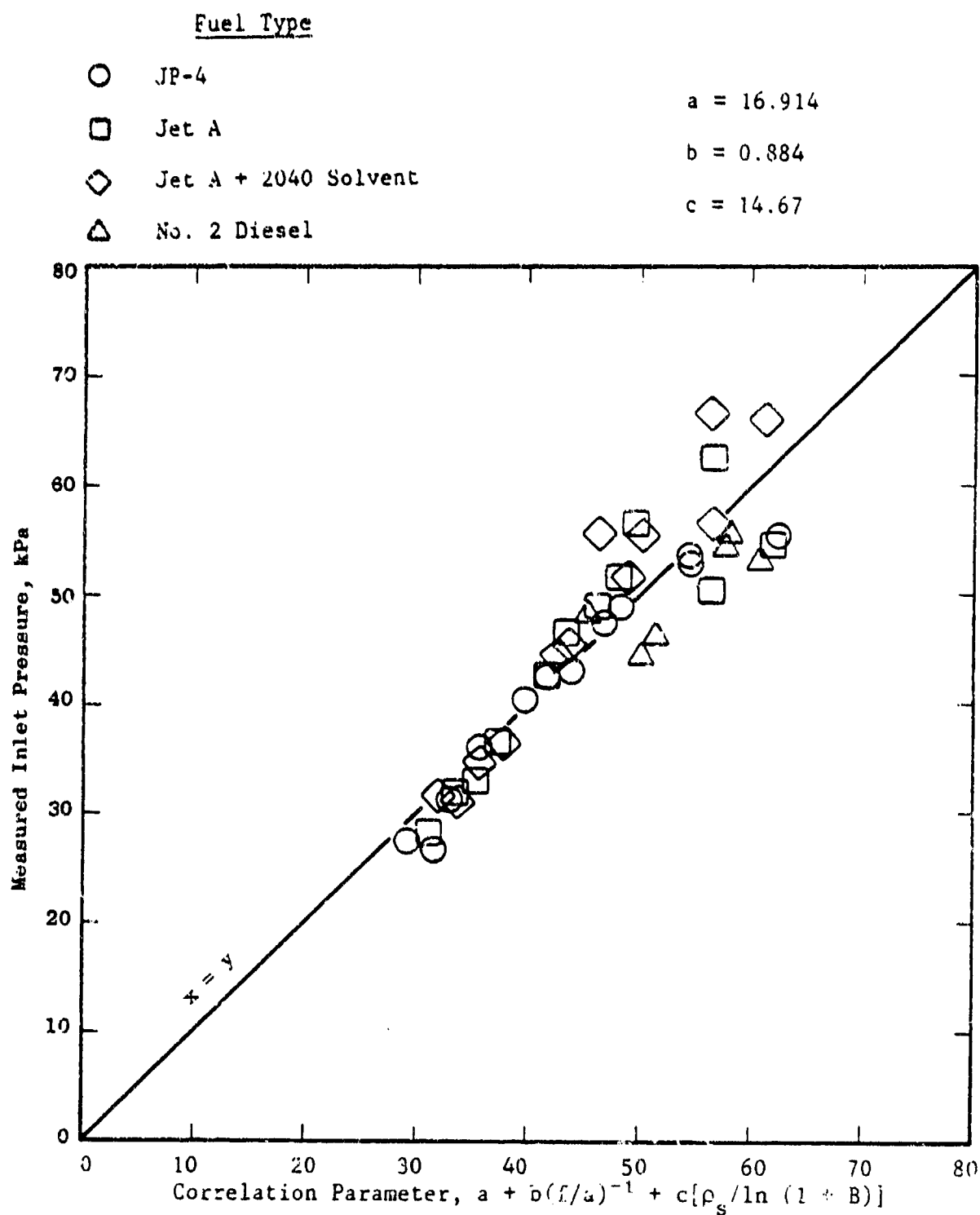


Figure 41. Pressure-Atomizing Nozzle Results; Complete-Blowout Correlation for All Fuels Tested.

only meaningful fuels comparison possible was the lightoff characteristics at ambient temperature.

The lightoff results for air-blast nozzles are shown in Figure 42. The volatility parameter $p_s/\ln(1+B)$ is plotted on the x-axis, and the combustor inlet total pressure for lightoff is the y-axis. This limited set of results seem to indicate that fuel volatility is rather important for ignition with air-blast nozzles. It is seen that JP-4 has a considerably smaller ignition threshold than Diesel 2.

The results for pressure-atomizing nozzles, where atomization effects were absent, indicate that there is a distinction between lightoff and full propagation. Also, there is a corresponding distinction between first-cup blowout and complete blowout. Fuel volatility has minor influence on initial lightoff and complete blowout but has no effect on full propagation and first-cup blowout. Such a distinction for ignition occurs in the three-phase theory of ignition (Reference 8). Lightoff and full propagation correspond to the first and second phases, respectively, of the analysis. The third phase concerns crossfiring in can-annular combustors and is not pertinent here.

Although the results have been presented in terms of the overall fuel/air ratio, the relevant parameter is the gas-phase fuel/air ratio in the vicinity of the ignition zone. However, the nature of the test matrix, which proved adequate for the intended purpose of fuel-property evaluation, did not permit separation of stoichiometry and dome velocity effects. It is suggested that further work along these lines would be fruitful in furthering understanding of the ignition and blowout processes.

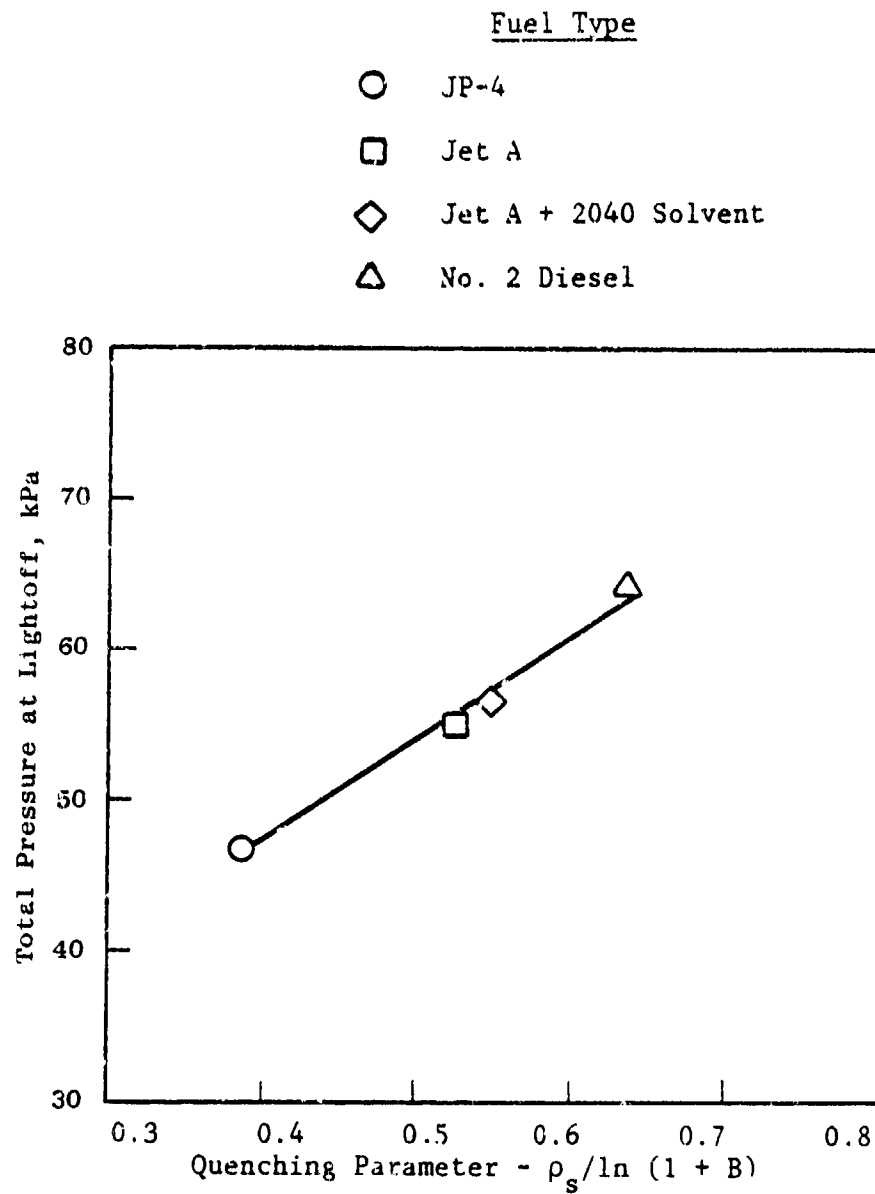


Figure 42. Lightoff Results for Air-Blast Nozzle.

7.0 CONCLUDING REMARKS

Previous studies of the effect of fuel properties on altitude relight and blowout characteristics of gas turbine engine combustors have established only the net effect of fuel-property variations. In particular, the effect of fuel physical properties such as viscosity, surface tension, and density (which govern the degree of atomization) was inseparable from the effect of fuel volatility since the same fuel nozzles were used for all the fuels. Distinguishing atomization effects from volatility effects in these studies was especially difficult since a highly volatile fuel such as JP-4 generally tends to also have superior atomizing characteristics for the same fuel-injection pressure. This investigation was undertaken to resolve the relative roles of atomization and volatility in determining the altitude relight characteristics of various fuels.

The experiments were conducted in a rectangular, five-swirl-cup combustor sector at inlet air temperatures and flows representing windmilling conditions of turbofan engines. Four fuels having widely varying volatility properties (JP-4, Jet A, a blend of Jet A and 2040 solvent, and Diesel 2) were used in the study. The effects of fuel properties on atomization were eliminated by using four matched sets of pressure-atomizing nozzles designed to give a spray Sauter mean diameter of $50 \pm 10 \mu\text{m}$ for each fuel at the same design fuel flow. A second series of tests was conducted with a single set of five prefilming air-blast nozzles which were not designed to give a particular SMD spray. Based on the test results, the following general conclusions emerge:

- It was possible to separate clearly the roles of atomization and volatility on the altitude-relight characteristics of four fuels spanning a wide range of volatility.
- When atomization effects were eliminated by achieving the same SMD for the different fuels, fuel volatility was found to play only a minor role in initial (first-cup) lightoff and complete blowout.
- The minor effect of fuel volatility on initial lightoff and complete blowout correlated well using a quenching parameter in which fuel volatility is represented by the transfer number.
- Full propagation (spreading of flame from initially lit swirl cup to all five cups) and first-cup blowout were essentially independent of fuel volatility and depended only on combustor operating conditions.
- Based on very limited data, it appears that air-blast nozzles give poorer ignition performance than the pressure-atomizing nozzles used in this program. Furthermore, they appeared to exhibit a stronger dependence of lightoff characteristics on volatility.
- This observed sensitivity to volatility for air-blast nozzles was also well correlated by the quenching parameter.

8.0 REFERENCES

1. Gleason, C.D., Oller, T.L., Shayeson, M.W., and Bahr, D.W., "Evaluation of Fuel Character Effects on J79 Engine Combustion System," AFAPL-TR-79-2015, 1979.
2. Gleason, C.C. et al., "Evaluation of Fuel Character Effects on the F101 Engine Combustion System," AFAPL-TR-79-2018, 1979.
3. Gleason, C.C. et al., "Evaluation of Fuel Character Effects on the J79 Smokeless Combustor," AFWAL-TR-80-2092, 1980.
4. Oller, T.L et al., "Fuel Mainburner/Turbine Effects," AFWAL-TR-81-2100, 1982.
5. Russel, P.L., "Fuel Mainburner/Turbine Effects," AFWAL-TR-81-2081, 1982.
6. Rosfjord, T.J., "Aviation Fuel Property Effects on Combustion," NASA CR-168334, 1984.
7. Kanury, A.M., Combustion Phenomena, Gordon and Breach, 1982.
8. Lefebvre, A.H., Gas Turbine Combustion, McGraw-Hill, 1983.
9. Lefebvre, A.H., "Fuel Effects on Gas Turbine Combustion," AFWAL-TR-83-2004, 1983.
10. Lefebvre, A.H., "Influence of Fuel Properties on Gas Turbine Combustion Performance," AFWAL-TR-2104, 1985.
11. Ballal, D.R. and Lefebvre, A.H., "Ignition and Flame Quenching of Quiescent Fuel Mists," Proc. R. Soc. London, Ser. A., Vol. 364, 1978.
12. Jasuja, A.K., "Atomization of Crude and Residual Fuel Oils," ASME Journal of Engineering for Power, Vol. 101, 1979.